SEQUENCE STRATIGRAPHY AND ARCHITECTURE OF LOWER PENNSYLVANIAN STRATA, SOUTHERN WEST VIRGINIA: POTENTIAL FOR CARBON SEQUESTRATION AND ENHANCED COAL-BED METHANE RECOVERY IN THE POCAHONTAS BASIN

William A. Rouse

Thesis submitted to the faculty of the Virginia Polytechnic Institute and State University in partial fulfillment of the requirements for the degree of

MASTER OF SCIENCE
in
GEOSCIENCES

Kenneth A. Eriksson, *Chair*
J. Fred Read
William S. Henika

August 29, 2009
Blacksburg, Virginia

Keywords: Lower Pennsylvanian, carbon sequestration, coal, methane, sequence stratigraphy

SEQUENCE STRATIGRAPHY AND ARCHITECTURE OF LOWER PENNSYLVANIAN STRATA, SOUTHERN WEST VIRGINIA: POTENTIAL FOR CARBON SEQUESTRATION AND ENHANCED COAL-BED METHANE RECOVERY IN THE POCAHONTAS BASIN

William A. Rouse

ABSTRACT

Carbon dioxide sequestration in coal-bed methane fields has potential to add significant recoverable reserves and extend the production life of coal-bed methane fields while at the same time providing a geologic sink for atmospheric greenhouse gases. The ability to relate the thickness, extent, and quality of coal seams to their relative position within a sequence is fundamental in determining the sequestration potential of a geologic formation. This thesis documents the carbon dioxide storage capacity and enhanced coal-bed methane recovery of lower Pennsylvanian coal-bearing siliciclastic strata within the Bradshaw CBM field, southern McDowell County, WV.

Analysis of outcrop, gamma ray and density logs, and eight cross-sections within the study area reveals a hierarchy of bounding discontinuities and architectural elements. Discontinuities are both erosional (unconformable) and depositional (condensed) surfaces of 3rd-order (~2.5 Ma) and 4th-order (~400 k.y.) origin. Architectural elements bound by 4th-order erosional discontinuities consist of upward-fining lowstand and transgressive incised valley fill, alluvial, and estuarine deposits, and upward-coarsening highstand deltaic deposits, representing 4th-order sequences. 4th-order sequences are stacked into composite 3rd-order sequences. Sequence development is attributed to higher frequency (~400 k.y.) 4th-order Milankovitch orbital eccentricity cycles superimposed on lower frequence (~2.5 Ma) orbital eccentricity cycles.

Coal seams occur in the transgressive and highstand systems tracts, associated with 4th-order flooding surfaces and high-frequency deltaic autocycles, respectively. Transgressive coal-bed development is attributed to Milankovitch driven glacio-eustacy while highstand coal-bed development is attributed to autocyclic deltaic influences.

Assessment of carbon dioxide storage capacity within coals of the lower Pennsylvanian Pocahontas and Bottom Creek formations in the Bradshaw CBM field indicates that 19 million tons of carbon dioxide can be sequestered. Sequestration of carbon dioxide within the Bradshaw CBM field has the potential to increase coal-bed methane recovery by as much as 52 billion cubic feet.

ACKNOWLEDGEMENTS

I would like to acknowledge my advisor, Ken Eriksson, who provided much needed guidance and support that was instrumental to my success at Virginia Tech. Additionally, I would like to thank my committee members, J. Fred Read and Bill Henika, for technical discussions and input that improved this thesis. I would also like to thank my colleagues Ryan Grimm, Tina Blue, and JoBeth Carbaugh for their support and unwavering friendship. Lastly, I would like to thank my family, for whom this thesis is dedicated.

CONTENTS

LIST OF FIGURES

TABLES

APPENDICES

1. INTRODUCTION

Concerns over climate change have prompted the development of carbon management strategies aimed at reducing levels of carbon dioxide in the atmosphere. One such strategy is carbon sequestration, a geoengineering technique where carbon dioxide is removed from the atmosphere and stored long-term in geologic, terrestrial, or oceanic reservoirs. A promising geologic reservoir for carbon dioxide storage is unminable coal seams, where carbon dioxide is adsorbed on the surface of coal while enhancing the recovery of coal-bed methane (CBM). Application of carbon sequestration to enhance the recovery of coal-bed methane allows for the utilization of unexploited mineral resources while reducing greenhouse gas emissions. The feasibility of such applications is highly dependent on the stratigraphy of the coal-bearing strata.

Coal thickness and quality are key factors in determining the viability of carbon sequestration and enhanced coal-bed methane (ECBM) production in coal seams. Coal thickness and extent has been shown to correlate with the position of the coal seam within a sequence, with the thickest and most extensive coals occurring in aggradational to slightly retrogradational stacking patterns associated with transgressive systems tracts (Bodek, 2006; Bohacs and Suter, 1997; Denning, 2008; Gibling et al., 2004). Coal quality (e.g. rank, mineral matter content) is the primary control on gas sorption capacity and sequestration potential of a coal seam (Pashin et al., 2002). The ability to relate the thickness, extent, and quality of coal seams to their relative position within a sequence is fundamental in determining the sequestration potential of a geologic formation.

Coal-bearing strata of the central Appalachian Basin have become an emergent CBM resource over the last decade, creating an extensive subsurface dataset of use in

developing a sequence stratigraphic framework. The lower Pennsylvanian Pocahontas Formation of the central Appalachian Basin contains interbedded coals and siliciclastics, including Pocahontas coals Nos. 1 through 7. The high concentration of coal seams within the formation, proximity of carbon dioxide sources in the form of coal-fired power plants, and occurrence of pre-existing CBM infrastructure make the Pocahontas Formation an attractive reservoir for carbon sequestration and ECBM.

2. PURPOSE AND SCOPE

The purpose of this paper is to 1) present a combined subsurface- and outcrop-based sequence stratigraphic framework for the Pocahontas Formation, 2) use this framework to relate the thickness, extent, and quality of coals to their position within sequences, 3) evaluate the carbon dioxide storage capacity within coal seams of the Pocahontas Formation, and 4) use the Pocahontas Formation as a type section to explore additional sequestration reservoirs in lower Pennsylvanian strata.

The Bradshaw CBM field in McDowell County, WV provides the ideal location and resolution for investigating the stratigraphy of coal-bearing siliciclastics of the Pocahontas Formation and for conducting detailed coal seam mapping. The Bradshaw CBM field (~25 km^2) is located along the border of McDowell County, WV and Buchanan County, VA (**Fig. 1**), a location that has been the target of extensive coal-bed methane production over the last 50 years. Digital subsurface data from the Bradshaw CBM field included both gamma ray and bulk density wireline logs, essential for identification of coals within the subsurface. Roadcuts along Route 10 near Garwood, WV expose the entire Pocahontas Formation, and were used in conjunction with

subsurface data from the Bradshaw CBM field in order to develop a sequence stratigraphic framework for the Pocahontas Formation (**Fig. 1)**. Additionally, outcrops along I-77 near the Camp Creek interchange, and Highwall Park near Bramwell, WV, were used to supplement subsurface data (**Fig. 1**).

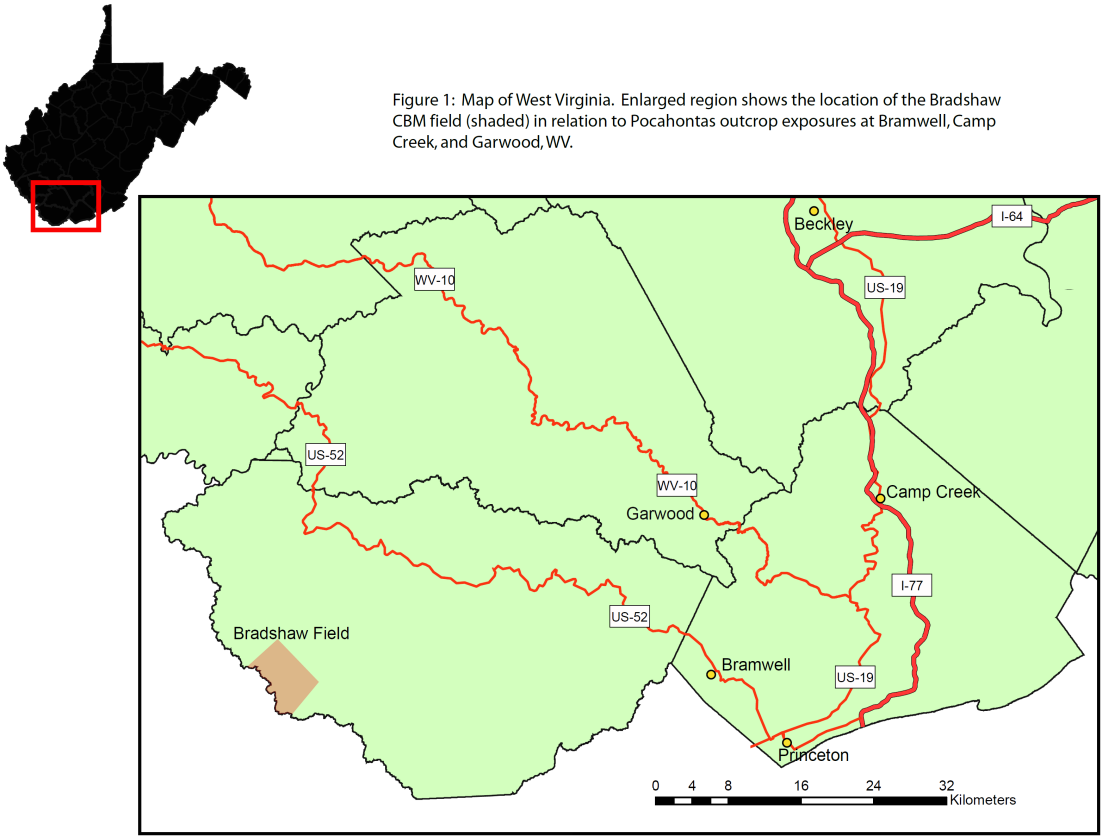

Figure 1: Map of West Virginia. Enlarged region shows the location of the Bradshaw CBM field (shaded) in relation to Pocahontas outcrop exposures at Bramwell, Camp Creek, and Garwood, WV.

3. GEOLOGIC BACKGROUND

3.1. Tectonic Setting

The Appalachian Basin is a northeast-southwest trending foreland basin which formed as a product of collisional tectonics from the combined effects of the Taconic, Acadian, and Alleghanian orogenies (Quinlan and Beaumont, 1984). The central

Appalachian Basin spans much of West Virginia, Virginia, Kentucky, and northeastern Tennessee, and is bound by five primary structures (**Fig. 2**). The Appalachian fold-and-thrust belt and the Cincinatti Arch define the southeastern and northwestern margins of the Appalachian Basin, respectively, while the Kentucky River Fault System, the Irvine-Paint Creek Fault System, and a structural hingeline in central West Virginia define the northern most extent of the basin (Greb and Martino, 2005). Basin accommodation for up to 9,500 ft of early Pennsylvanian through early Permian terrestrial and marginal-marine siliciclastics rocks was provided by subsidence due to thrust loading of the Appalachian fold-and-thrust belt during the Alleghanian orogeny (Ettensohn, 2004; Rice and Schwietering, 1988).

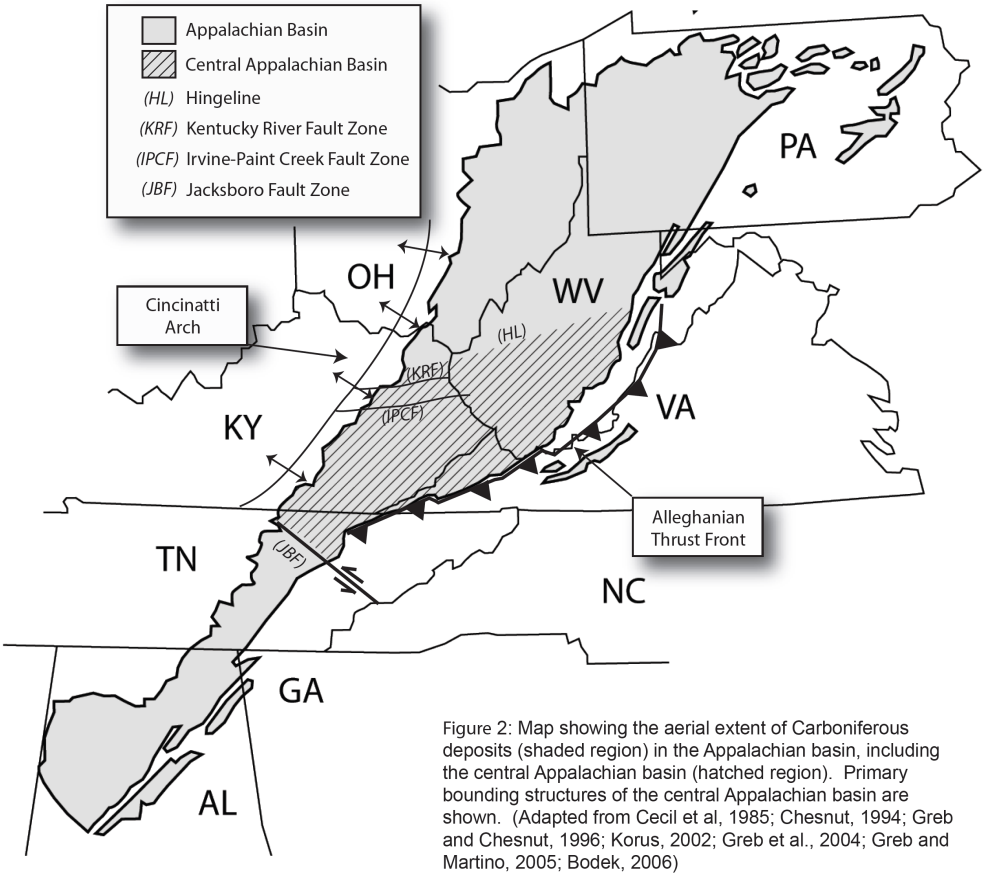

Figure 2: Map showing the aerial extent of Carboniferous deposits (shaded region) in the Appalachian basin, including the central Appalachian basin (hatched region). Primary bounding structures of the central Appalachian basin are shown. (Adapted from Cecil et al, 1985; Chesnut, 1994; Greb and Chesnut, 1996; Korus, 2002; Greb et al., 2004; Greb and Martino, 2005; Bodek, 2006)

3.2. Carboniferous Stratigraphy

Carboniferous strata of lower and middle Pennsylvanian age are arranged in two interfingering facies belts; a southeastern facies belt consisting of mixed siliciclastics, coal-bearing strata, and a northwestern facies belt comprised mainly of quartzarenite sandstone bodies (**Fig. 3**; Englund, 1974).

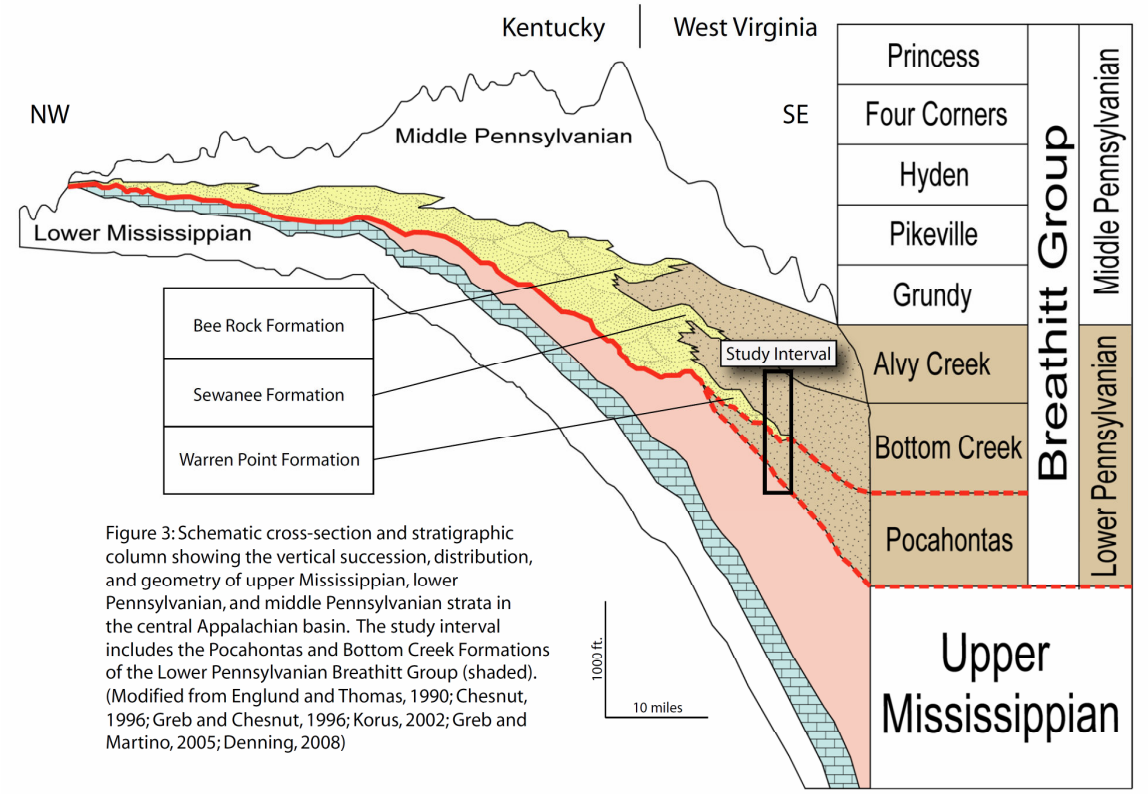

Figure 3: Schematic cross-section and stratigraphic column showing the vertical succession, distribution, and geometry of upper Mississippian, lower Pennsylvanian, and middle Pennsylvanian strata in the central Appalachian basin. The study interval includes the Pocahontas and Bottom Creek Formations of the Lower Pennsylvanian Breathitt Group (shaded). (Modified from Englund and Thomas, 1990; Chesnut, 1996; Greb and Chesnut, 1996; Korus, 2002; Greb and Martino, 2005; Denning, 2008)

Coal-bearing siliciclastic strata of the lower and middle Pennsylvanian Breathitt Group consist primarily of northwest-trending sublithic sandstone bodies with sediment derived from the low-grade metamorphic terrain of the Alleghanian orogen, with lesser amounts of siltstone, shale, underclay, and coal (Englund et al., 1986; Rice, 1985; Rice and Schwietering, 1988). The Breathitt clastic wedge thickens toward the thrust-loaded hinterland, with a maximum thickness of ~2400 ft along the southeast margin of the basin

(Chesnut, 1996; Chesnut, 1994; Englund et al., 1979; Englund and Thomas, 1990; Korus, 2002).

Quartzarenite sandstones of the lower and middle Pennsylvanian Breathitt Group occur as northeast-southwest oriented bodies that are lenticular in cross-section, 37-50 miles wide (Greb et al., 2004), up to 500 feet thick and typically are made up of thinner (70-100 feet thick) individual quartzarenite beds (Chesnut, 1996; Chesnut, 1994). Quartzarenites within the northwestern facies belt have southwesterly paleoflow and are arranged *en echelon*, onlapping and amalgamating cratonward (Greb et al., 2004; Greb and Chesnut, 1996; Wizevich, 1992). Quartzarenites within the northwestern facies belt bifurcate, pinch-out, and grade laterally into the coal-bearing siliciclastic belt toward the southeast (**Fig. 3**).

3.3. Lower Pennsylvanian Lithostratigraphic Nomenclature

3.3.1 Formalized Kentucky Nomenclature

Stratigraphic nomenclature used in this paper corresponds to formalized Kentucky nomenclature (Bodek, 2006; Chesnut, 1996; Chesnut, 1994). The lower Pennsylvanian Breathitt Group consists of, in ascending order, the Pocahontas, Bottom Creek, and Alvy Creek Formations (**Fig. 4**). These formations are separated by widespread marine horizons (Chesnut, 1996; Chesnut, 1994). The southeastern facies belt of the Breathitt Group is composed primarily of texturally and mineralogically immature siliciclastics and intercalated coal beds, while the northwestern facies belt consists of quartzarenite formations equivalent to the Pocahontas, Bottom Creek, and Alvy Creek Formations.

These quartzarenites are, in ascending order, the Warren Point, Sewanee, and Bee Rock Formations of the Breathitt Group (**Fig. 4**; Chesnut, 1994; Greb et al., 2004).

3.3.2. Correlation into West Virginia

In West Virginia, coal-bearing units of the Bottom Creek and Alvy Creek Formations of the southeastern facies belt are combined into the New River Formation (Korus, 2002). Quartzarenites dominate the northwestern facies belt of the New River Formation, and are collectively known as the 'Salt Sands.' Individual quartzarenite sand bodies within the 'Salt Sands' include the Lower Raleigh, Upper Raleigh, and Guyandot, equivalent to the Sewanee Formation in Kentucky, and the Pineville, equivalent to the Warren Point Formation in Kentucky. The Bee Rock Formation in Kentucky correlates to the Nuttall Member in West Virginia.

3.4. Lower Pennsylvanian Global Correlations

The Carboniferous Period was subdivided in 1975 by the Eighth International Congress on Carboniferous Stratigraphy and Geology (Congress, 1975) into early, middle, and upper periods to aid in global correlations between established Russian stages and North American stratotypes (Davydov et al., 2004). Lower Pennsylvanian period is equivalent to the International (Russian) Bashkirian Stage, European Namurian B through Westphalian B Stages, and North American Morrowan through Lower Atokan Stages (**Fig. 4**; Davydov et al., 2004). Radiometric dating constrains the base of the lower Pennsylvanian at 318.1 +/- 1.3 m.y. and lower – middle Pennsylvanian boundary at

311.7 +/- 1.1 m.y., resulting in a mean duration for the lower Pennsylvanian of 6.4 m.y. (Bodek, 2006).

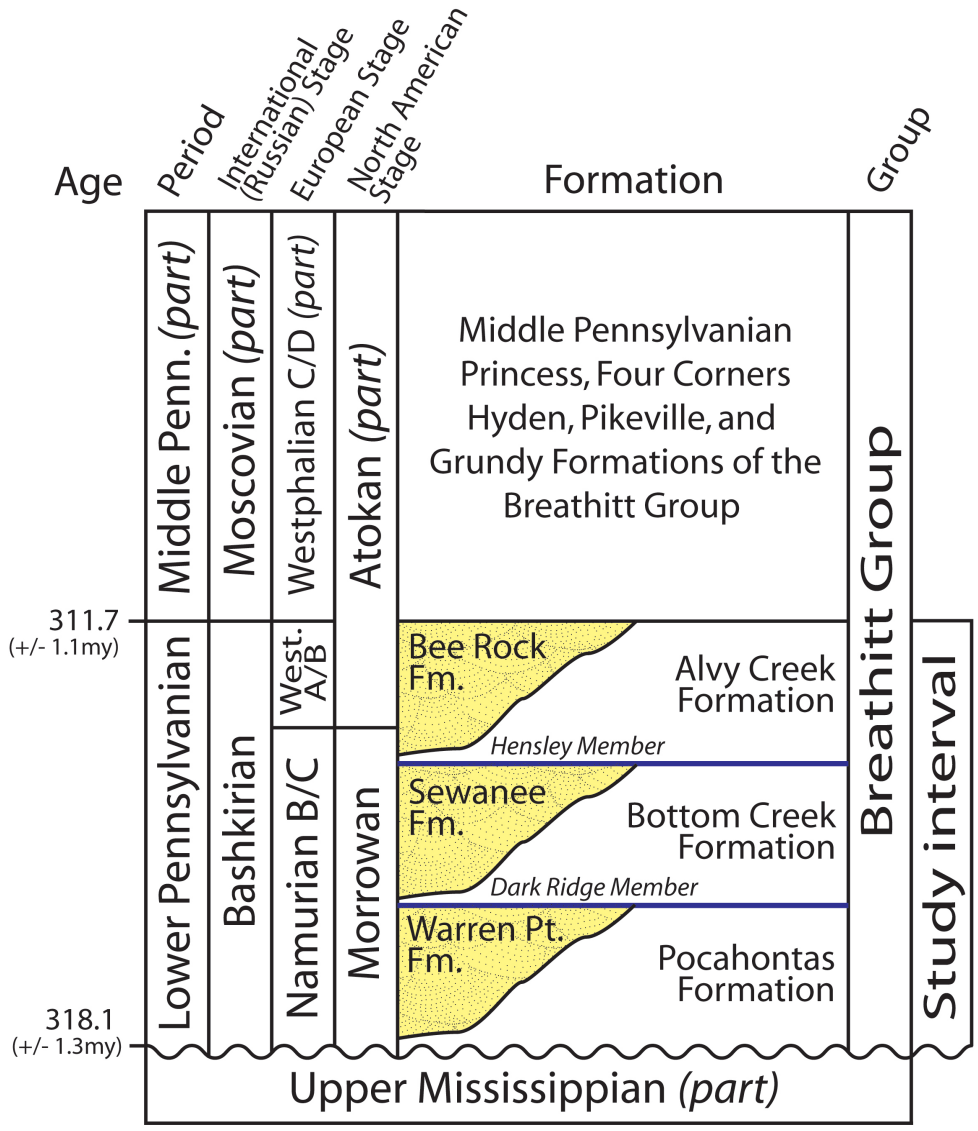

Figure 4: Stratigraphic relationship of lower and middle Pennsylvanian strata in the central Appalachian basin to period and global stage boundaries. Note age estimates for the upper and lower boundaries of the lower Pennsylvanian period (Bashkirian Stage) (Davydov et al., 2004). (Modified from Chesnut, 1994; Bodek, 2006; Denning, 2008).

3.5. Depositional Setting

Numerous depositional models have been developed to explain the stratal relationships of lower Pennsylvanian Breathitt quartzarenites and juxtaposed coal-bearing

siliciclastic strata (see reviews in Bodek (2006) and Denning (2008). A trunk-tributary depositional model has gained popularity in recent time by accommodating the coeval facies of the northwestern and southeastern facies belts. The trunk-tributary model describes the interaction of two fluvial systems draining different terrains. During sea level lowstands, westerly flowing tributary rivers drained the southeastern Appalachian fold-and-thrust belt (Rice and Schwietering, 1988), merging into large, bedload-dominated braided trunk rivers carrying quartzose bedload down the axis of the Appalachian foreland from the Canadian Shield (Archer and Greb, 1995; Bodek, 2006; Denning, 2008; Greb and Chesnut, 1996; Korus, 2002). During subsequent sea level rise, the fluvial systems were transgressed, resulting in drowning of trunk and tributary incised valleys and the formation of estuaries (Bodek, 2006; Greb and Chesnut, 1996; Greb and Martino, 2005; Korus, 2002). Coal beds associated with estuaries formed in response to sea level rise. A decrease in the rate of relative sea level rise resulted in the progradation of bay-head deltas into the estuaries, forming coarsening-upward parasequences at sea level highstand. Coal beds associated with coarsening-upward parasequences formed in response to periodic abandonment of delta lobes due to compaction-induced subsidence (Denning, 2008). A fall in sea level followed bay-head delta formation, resulting in incision and the beginning of another cycle of eustatic sea level change.

3.6. Sequence Stratigraphy of Lower Pennsylvanian Coal-Bearing Strata

Lower Pennsylvanian coal-bearing strata occur in cyclic packages known as ‘cyclothems’ (Wanless and Shepard, 1936; Weller, 1930). These cyclothems have been

described in both a genetic (Chesnut, 1994; Galloway, 1989) and a depositional context (Aitken and Flint, 1994; Heckel et al., 1998).

Genetic classification identifies cyclothems bound by coals, referred to as a 'coal-clastic' cycle (Chesnut, 1994). A typical genetic cyclothem starts at the top of a major coal seam which is overlain by an upward-coarsening succession of mudstone, heterolithic, and sandstone, which is in turn overlain by a upward-fining succession beginning with cross-bedded sandstone and fining upwards to a rooted paleosol, capped with another major coal that marks the top of the genetic cyclothemic succession (Chesnut, 1994). A widespread disconformity separates the upward-coarsening from upward-fining succession, demarcated by either an erosionally based channel-fill sandstone or interfluve paleosol (Chesnut, 1994). Depositional classification identifies cyclothems bounded by the aforementioned widespread disconformities, or sequence boundaries (Aitken and Flint, 1994; Heckel et al., 1998).

Using the genetic classification of a cyclothem, seven major marine zones were identified in the Breathitt Group, subdividing the group into eight formations of approximate equal thickness and duration (Chesnut, 1994; Greb et al., 2004). The major marine zones were suggested to mark the peak of major transgressive cycles with duration of 2.5 m.y., representing a maximum flooding surface (Chesnut, 1994). Five to six coal-clastic cycles occur within each major transgressive cycle, with an estimated duration of 400 k.y. each (Greb et al., 2004). Major transgressive cycles of 2.5 m.y. were attributed to post-tectonic marine incursions following foreland basin subsidence during the Alleghanian orogeny (Chesnut, 1994; Quinlan and Beaumont, 1984). Coal-clastic

cycles of 400 k.y. were attributed to long-term Milankovitch orbital eccentricity (Chesnut, 1994).

Recent work has utilized the depositional classification for lower Pennsylvanian cyclothems. Bodek (2006) and Denning (2008) identified both major and minor sequence boundaries in lower Pennsylvanian strata, located some distance beneath 3rd-order maximum flooding surfaces and minor flooding zones, respectively. Bodek (2006) identified 18 minor sequence boundaries within the lower Pennsylvanian of the central Appalachian Basin, corresponding to 4th-order orbital eccentricity cycles (Plint et al., 1992; Read, 1995). Third-order composites sequences are comprised of stacked 4th-order sequences, and have been suggested to represent lower-frequency orbital eccentricity cycles of ~2.5 m.y. periodicity (Bodek, 2006).

4. METHODOLOGY

Subsurface and outcrop data were combined to develop a three-dimensional sequence stratigraphic framework for the Pocahontas Formation for use in evaluating the sequestration potential of lower Pennsylvanian strata.

4.1. Outcrop Studies

Roadcuts and abandoned mine walls were used in surface investigations of the Pocahontas Formation. Roadcuts located along Route 10, east of Garwood, WV exposes the entire Pocahontas interval with over 500 ft of outcrop (Figure 5; Appendix A). Roadcuts along I-77 near the Camp Creek Interchange expose the Pocahontas 1 sandstone body, the Pocahontas #2 coal, and the Warren Point

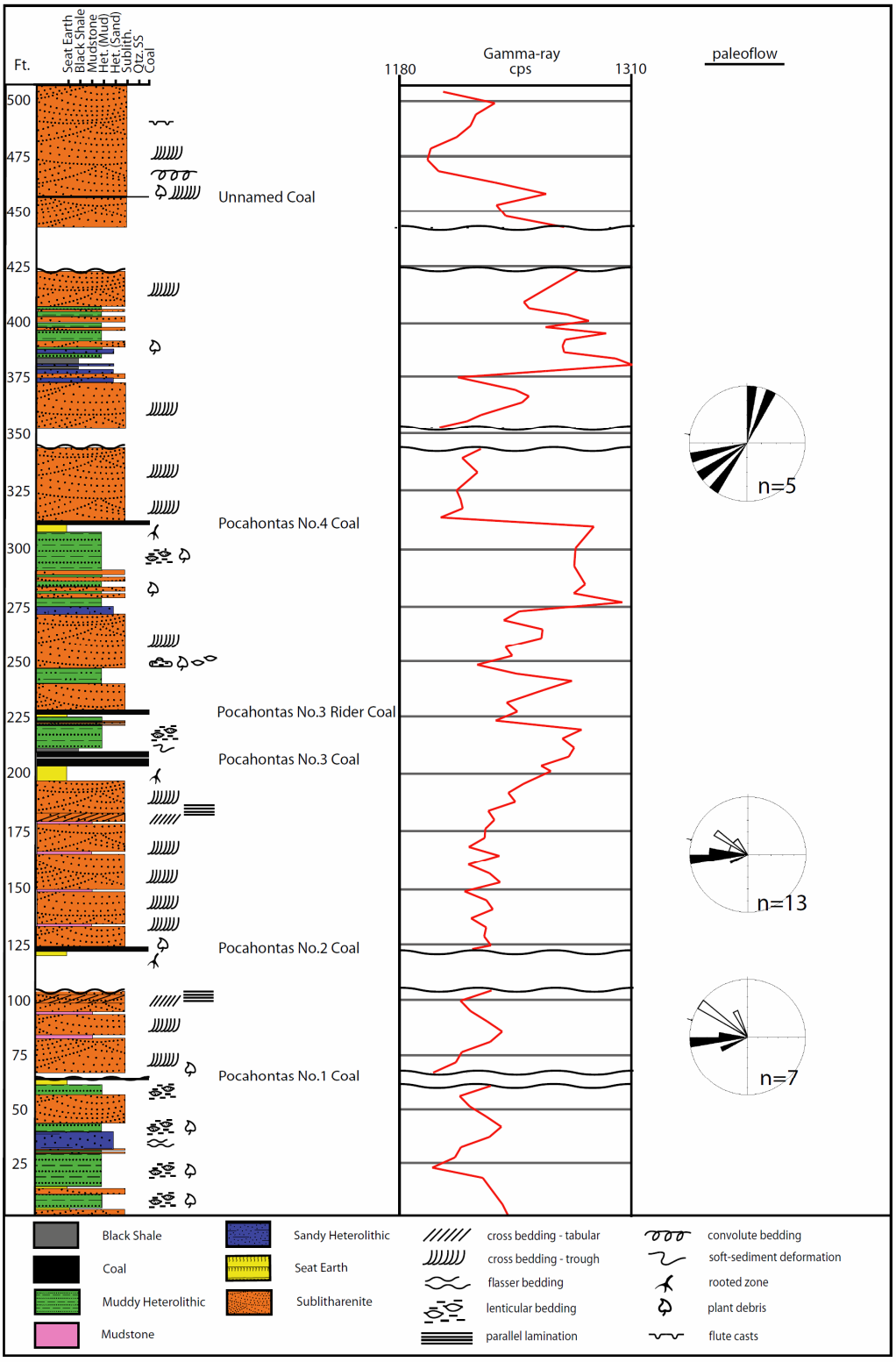

Figure 5. Stratigraphic column and gamma-ray response of Pocahontas Formation exposed along State Route 10 near Garwood, West Virginia - most complete exposure of Pocahontas Formation (Englund et al., 1979). Paleoflow direction is from trough (black) and planar (white) cross-beds. See Appendix A for enlarged version of this column.

Formation. An abandoned mine wall at Highwall Park near Bramwell, WV, exposes the stratigraphic interval between the base of the Pocahontas #6 coal-bed and 20 feet above the Pocahontas #6 Rider coal-bed (**Appendix B)**. Both I-77 and Bramwell, WV outcrop localities were used to supplement the more extensive Garwood, WV section.

4.1.1. Photomosaics

Photomosaics were constructed for each of the three roadcut localities along I-77 (**Appendix C**). Photomosaics were created from 40+ digital images merged together using Adobe Photoshop's *Photomerge* feature. These images were then overlain with detailed outcrop descriptions.

4.1.2. Spectral gamma-ray scintillometer

Almost all natural gamma radiation attributed to the radioactivity of rocks originates from the decay of three radionuclides; ^{40}K, ^{238}U, and ^{232}Th (Myers and Wignall, 1987). During radioactive decay, these elements emit high-energy gamma radiation whose energy is characteristic of the emitting isotope (Myers and Wignall, 1987). By measuring the intensity and energy of gamma radiation at a particular location, one can determine the abundance of K, U, and Th (Myers and Wignall, 1987).

Measurement of these radionuclides with a gamma-ray scintillometer is both direct and indirect. Potassium emits a single gamma-ray (^{40}K) with the energy of 1.461 megaelectron volts (MeV), making the determination of K a direct one (GF Instruments, 2000). ^{238}U and ^{232}Th series each emit a multitude of gamma rays of different energies, of which only one is measured by the detector (Myers and Wignall, 1987). In this study,

the determination of the concentration of U is based on the detection of ^{214}Bi radionuclide which is part of the ^{238}U decay series emitting the energy of 1.764 MeV (Instruments, 2000). Uranium detection is thus indirect, given as eU (equivalent of uranium). Determination of Th is also indirect (eTh), based on the detection of ^{208}Tl radionuclide which is part of the ^{232}Th decay series emitting the energy of 1.764 MeV (Instruments, 2000). Concentration of K, eU, and eTh is measured by counting the number of emitted gamma-rays within the energy frequencies noted above, recorded as counts per second (cps).

Gamma-ray logs were obtained on measured sections of the Pocahontas Formation using a handheld GRS-2000 Multispec spectral gamma-ray scintillometer (**Fig. 5; Appendix A**). Readings were taken at 5 ft intervals, recording total spectral counts as well as counts for K, U, and Th spectral bands.

4.2. Subsurface Studies

This study focuses on a coal-bed methane reservoir (Bradshaw CBM Field) located at the southern border of McDowell county, West Virginia (**Fig. 1**). The Bradshaw CBM Field consists of 80+ coal-bed methane wells of use in the characterization of lower Pennsylvanian strata. A majority of the CBM wells have both gamma ray and density wire-line log data through the entire lower Pennsylvanian section.

In addition to CBM well-log data in the Bradshaw CBM Field, a suite of conventional well-log data is used to delineate the extent of the Pocahontas Formation within the central Appalachian Basin of southern West Virginia. Conventional wells are generally deeper than CBM wells, enabling identification of the contact dividing the

Mississippian and Pennsylvanian systems. However, while CBM wells are shallower than conventional wells, the density record allows for accurate identification of coal seams and splits. Thus, for a complete subsurface study of the lower Pennsylvanian in the central Appalachian Basin, both CBM and conventional well-logs must be utilized.

4.2.1. Construction of cross-sections

Eight cross-sections from southern West Virginia were constructed using Haliburton's Geographix XSection software in order to characterize lower Pennsylvanian strata in detail (**Fig. 6**). Regional cross-section R-R' oriented parallel to structural dip of the basin illustrates the relationships between the northwest quartzarenite facies belt and southeast sublitharenite facies belt (**Fig. 7**). This regional cross-section was hung on the Hensley Shale Member (**Fig. 4;** maximum marine flooding surface).

Seven high-resolution cross-sections were constructed in the Bradshaw CBM field. Coal-bed methane well data in the Bradshaw field contain both gamma-ray and density log data for a majority of the wells. Each cross section contains between 8 and 11 data points with log spacing between 0.24 and 1.5 kilometers. Four cross-sections were oriented parallel to structural strike of the basin (A-A', B-B', C-C', D-D'; **Figs. 8-11**), whereas three cross-sections were oriented along structural dip of the basin (E-E', F-F', G-G'; **Figs. 12-14**). Cross-sections were oriented such that they had common intersecting well points. All cross-sections were hung on a common datum. While previous researchers have used the Hensley Shale Member maximum marine flooding unit as their datum (Bodek, 2006; Denning, 2008; Greb and Chesnut, 1992), it was found that many of the well-logs started at depths lower than the base of the Hensley Shale.

This study therefore uses the Dark Ridge Shale Member (**Fig. 4;** maximum flooding surface) as the datum for Bradshaw CBM field cross-sections, due to its regional extent and presence in all well logs in the area of interest.

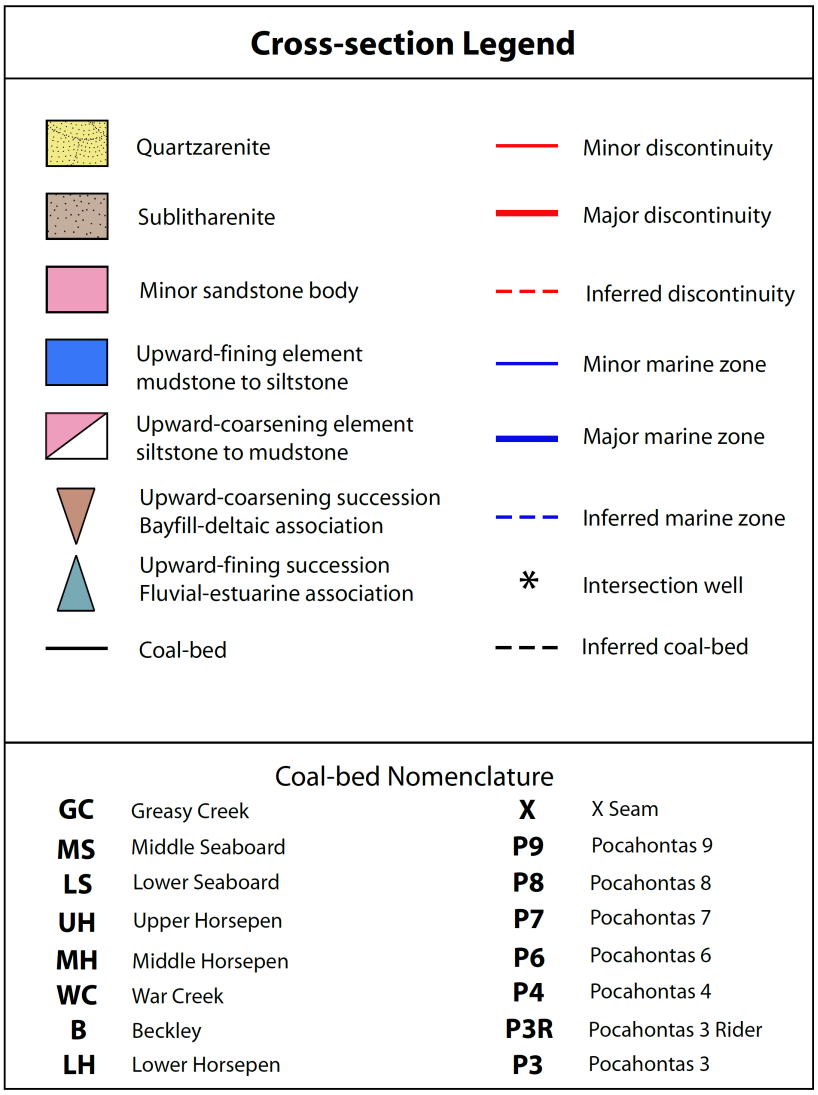

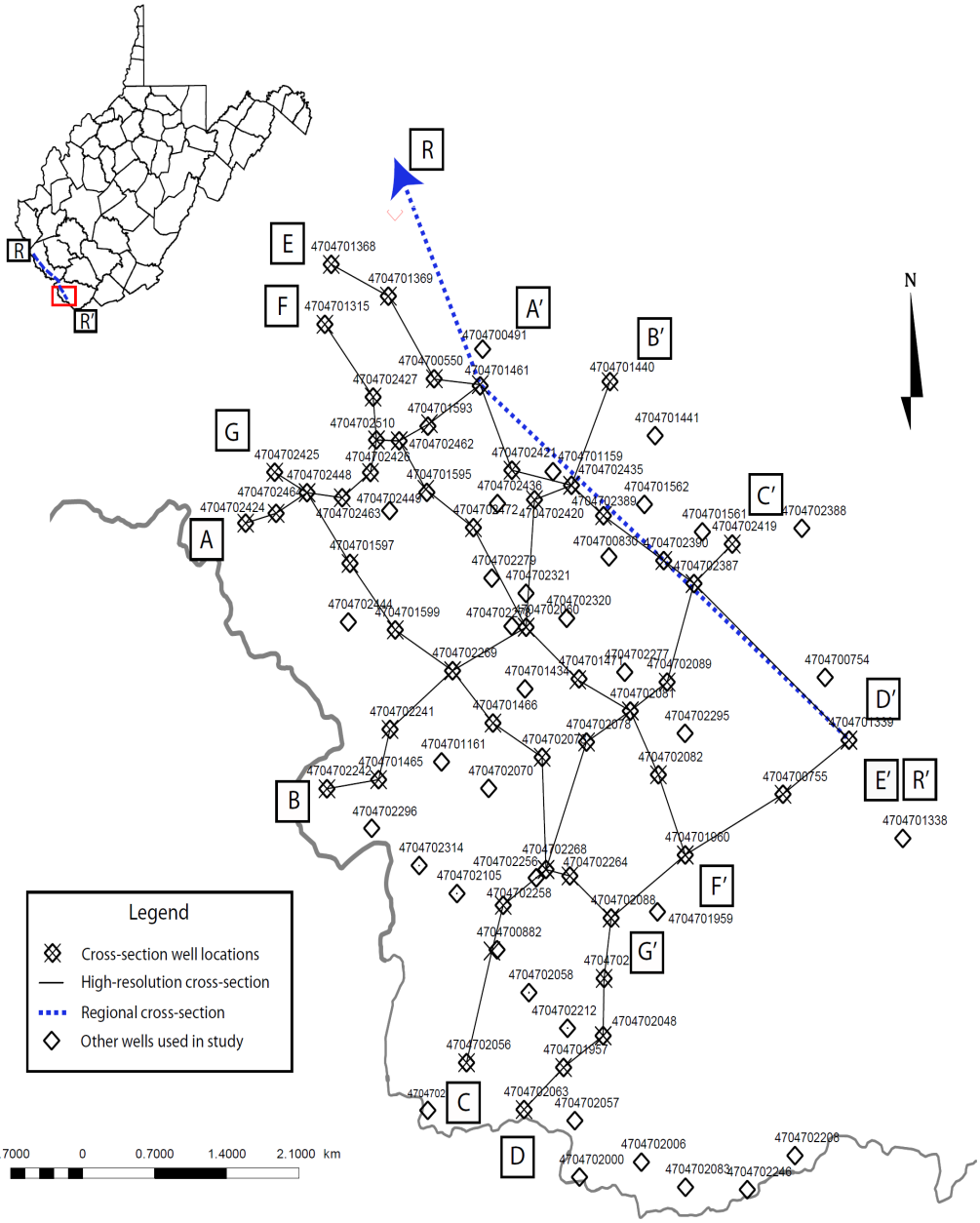

Figure 6. Map of West Virginia showing locations of cross-sections within the study area. Enlarged area shows spatial location of well data points used to construct strike-oriented cross-sections (A-A', B-B', C-C', and D-D') and dip-oriented cross-sections (E-E', F-F', G-G', and R-R').

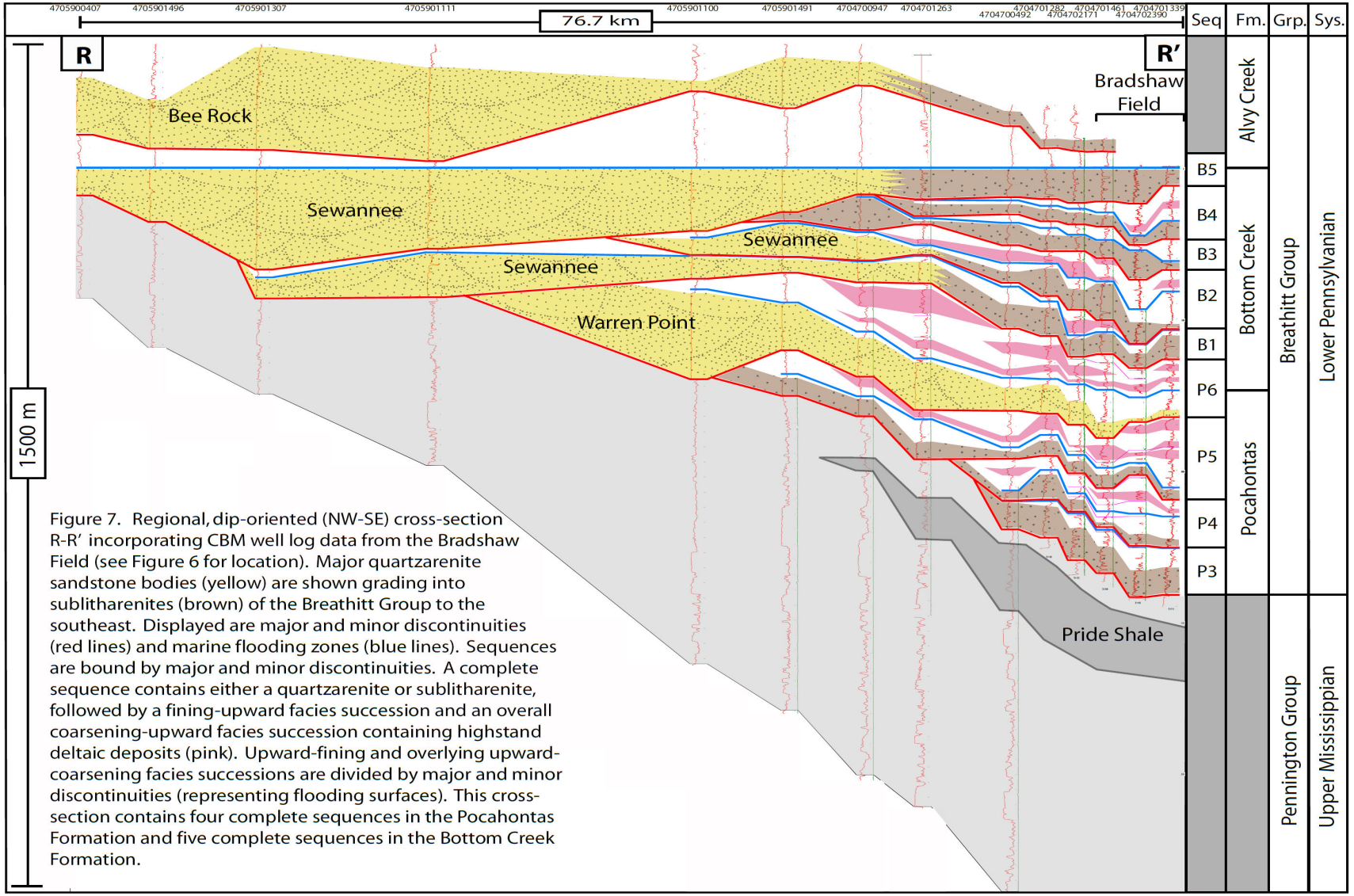

Figure 7. Regional, dip-oriented (NW-SE) cross-section R-R′ incorporating CBM well log data from the Bradshaw Field (see Figure 6 for location). Major quartzarenite sandstone bodies (yellow) are shown grading into sublitharenites (brown) of the Breathitt Group to the southeast. Displayed are major and minor discontinuities (red lines) and marine flooding zones (blue lines). Sequences are bound by major and minor discontinuities. A complete sequence contains either a quartzarenite or sublitharenite, followed by a fining-upward facies succession and an overall coarsening-upward facies succession containing highstand deltaic deposits (pink). Upward-fining and overlying upward-coarsening facies successions are divided by major and minor discontinuities (representing flooding surfaces). This cross-section contains four complete sequences in the Pocahontas Formation and five complete sequences in the Bottom Creek Formation.

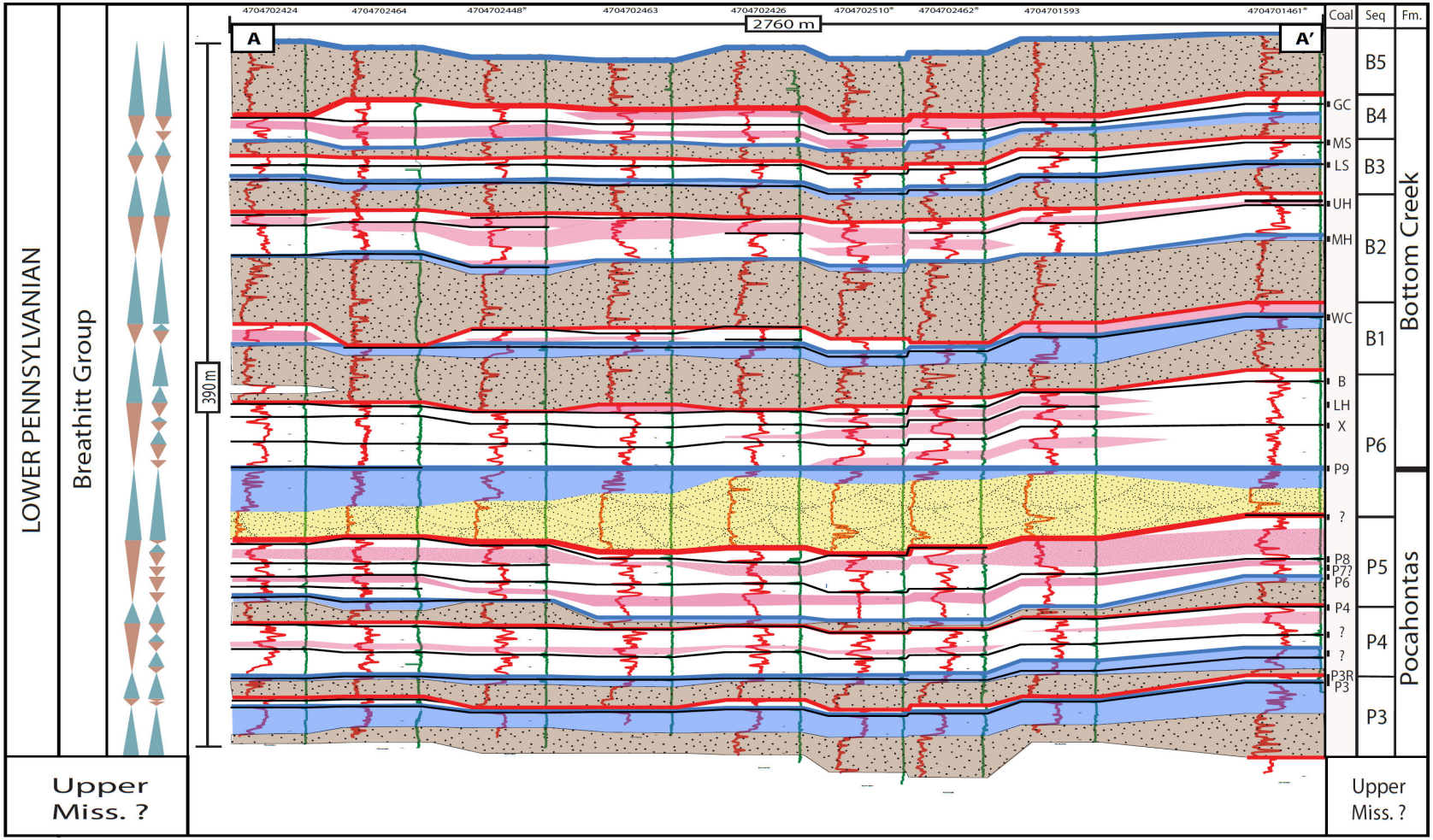

Figure 8. Strike-oriented (SW-NE) cross-section A-A' (see Figure 6 for location). Displayed are minor discontinuities (thin red lines), major disontinuities (thick red lines), minor marine zones (thin blue lines), and major marine zones (thick blue lines). Sequences are bound by minor and major discontinuities. A complete sequence contains either quartzarenite (yellow) or sublitharenite (brown), followed by light blue fining-upward fluvial-estuarine facies and red coarsening-upward bay-fill deltaic facies. This cross-section displays 4 sequences in the Pocahontas formation and 5 sequences in the Bottom Creek Formation.

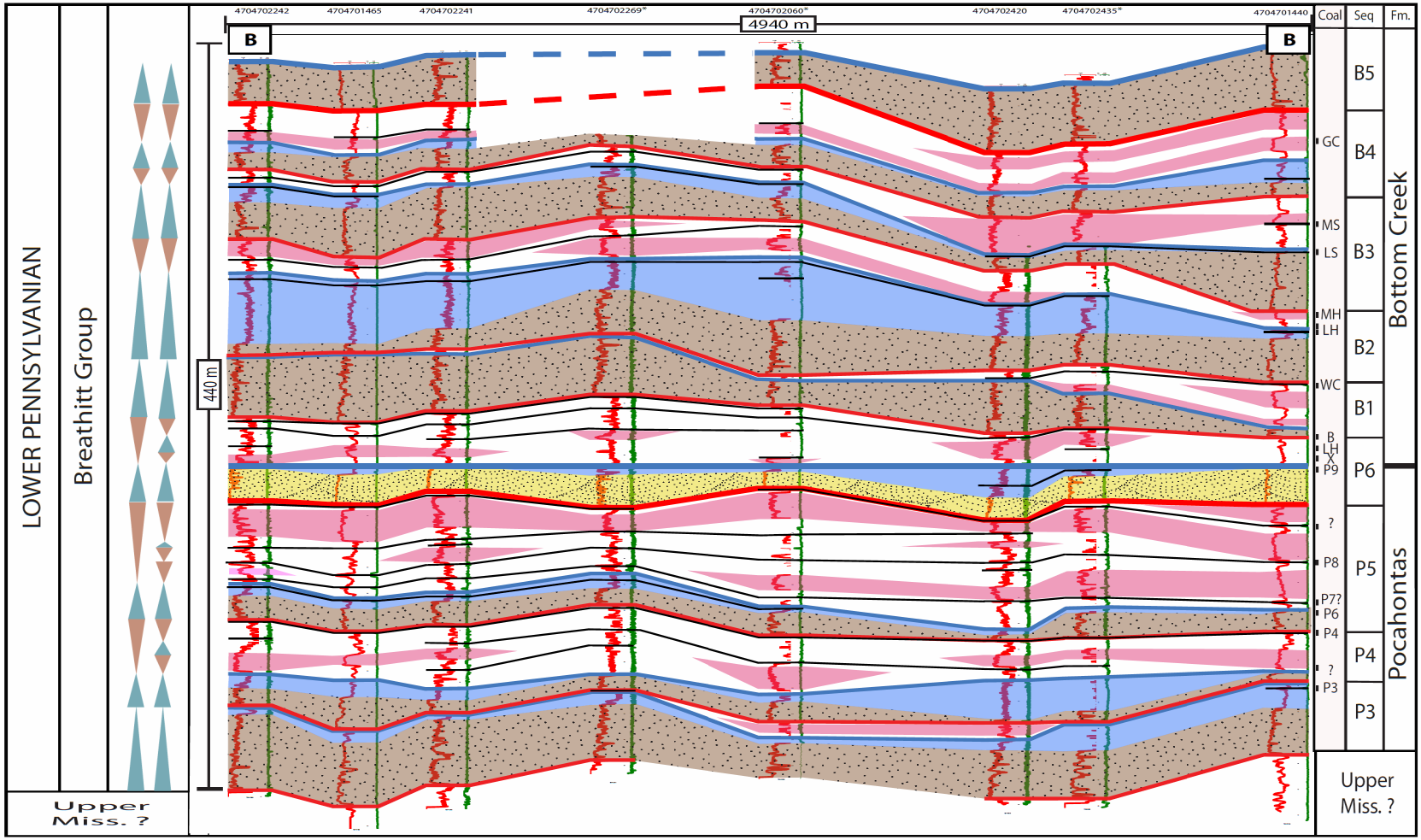

Figure 10. Strike-oriented (SW-NE) cross-section C-C' (see Figure 6 for location). Displayed are minor discontinuities (thin red lines), major disontinuities (thick red lines), minor marine zones (thin blue lines), and major marine zones (thick blue lines). Sequences are bound by minor and major discontinuities. A complete sequence contains either quartzarenite (yellow) or sublitharenite (brown), followed by light blue fining-upward fluvial-estuarine facies and red coarsening-upward bay-fill deltaic facies. This cross-section displays 4 sequences in the Pocahontas formation and 5 sequences in the Bottom Creek Formation.

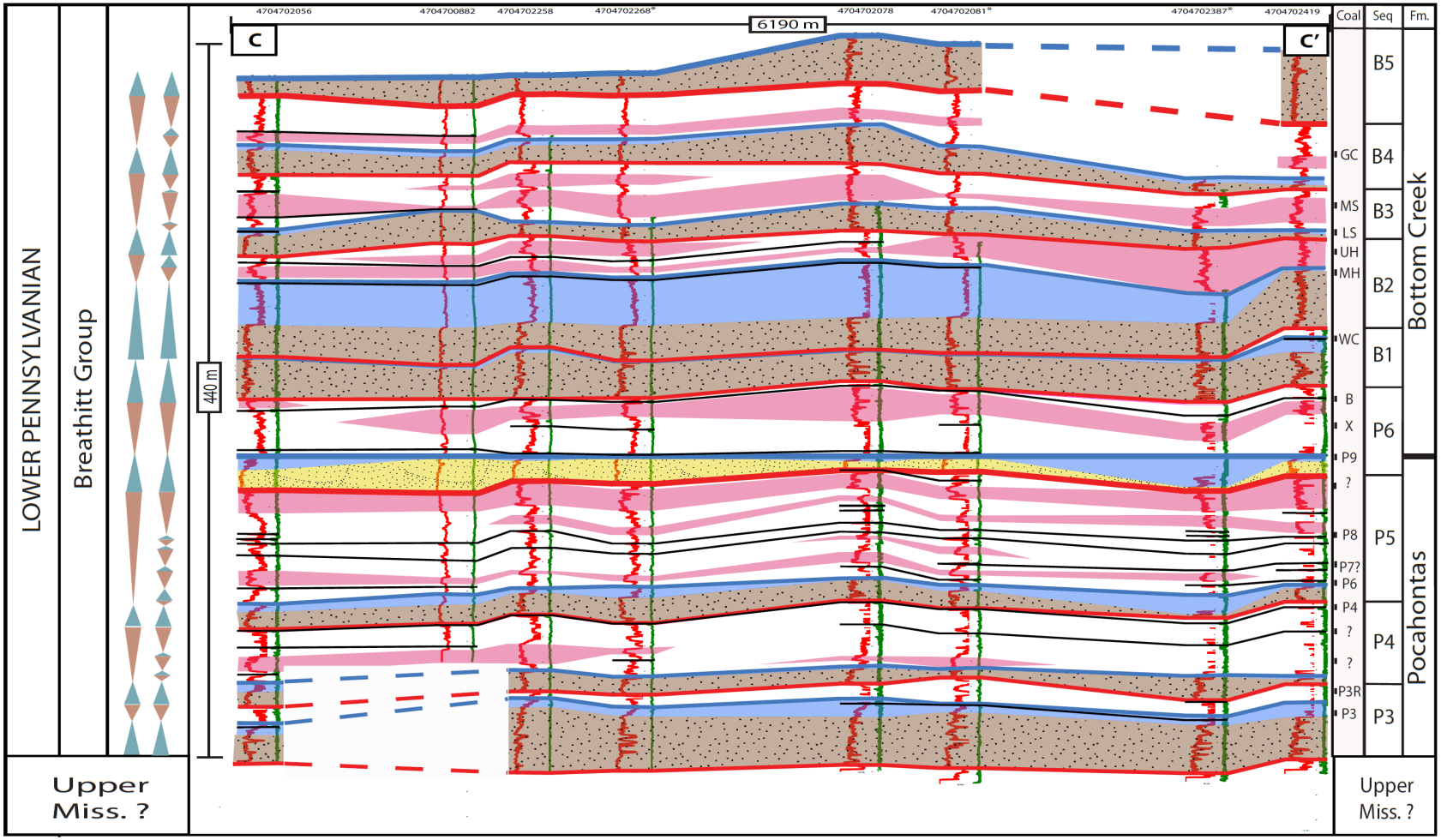

Figure 10. Strike-oriented (SW-NE) cross-section C-C′ (see Figure 6 for location). Displayed are minor discontinuities (thin red lines), major disontinuities (thick red lines), minor marine zones (thin blue lines), and major marine zones (thick blue lines). Sequences are bound by minor and major discontinuities. A complete sequence contains either quartzarenite (yellow) or sublitharenite (brown), followed by light blue fining-upward fluvial-estuarine facies and red coarsening-upward bay-fill deltaic facies. This cross-section displays 4 sequences in the Pocahontas formation and 5 sequences in the Bottom Creek Formation.

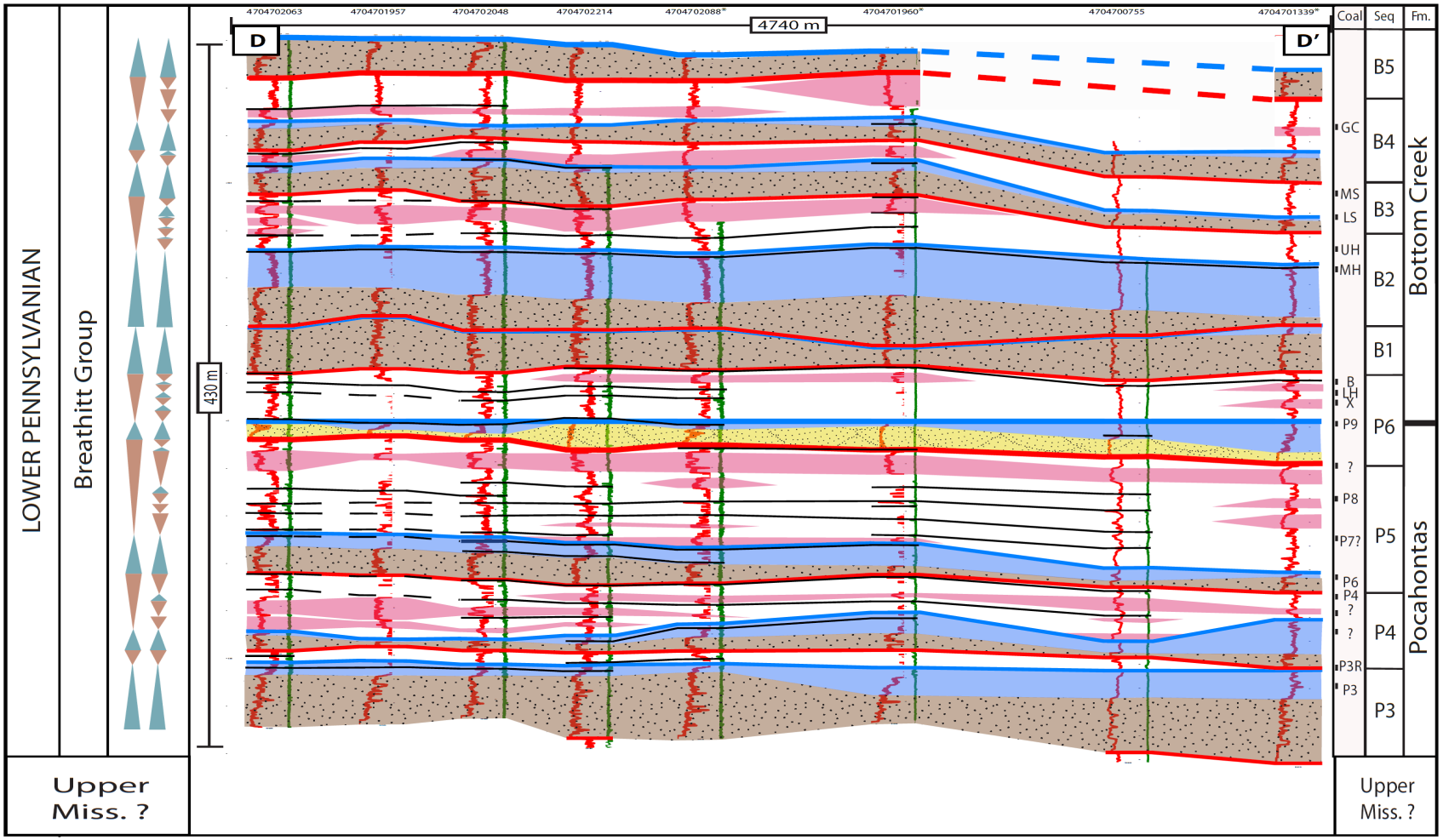

Figure 11. Strike-oriented (SW-NE) cross-section D-D' (see Figure 6 for location). Displayed are minor discontinuities (thin red lines), major disontinuities (thick red lines), minor marine zones (thin blue lines), and major marine zones (thick blue lines). Sequences are bound by minor and major discontinuities. A complete sequence contains either quartzarenite (yellow) or sublitharenite (brown), followed by light blue fining-upward fluvial-estuarine facies and red coarsening-upward bay-fill deltaic facies. This cross-section displays 4 sequences in the Pocahontas formation and 5 sequences in the Bottom Creek Formation.

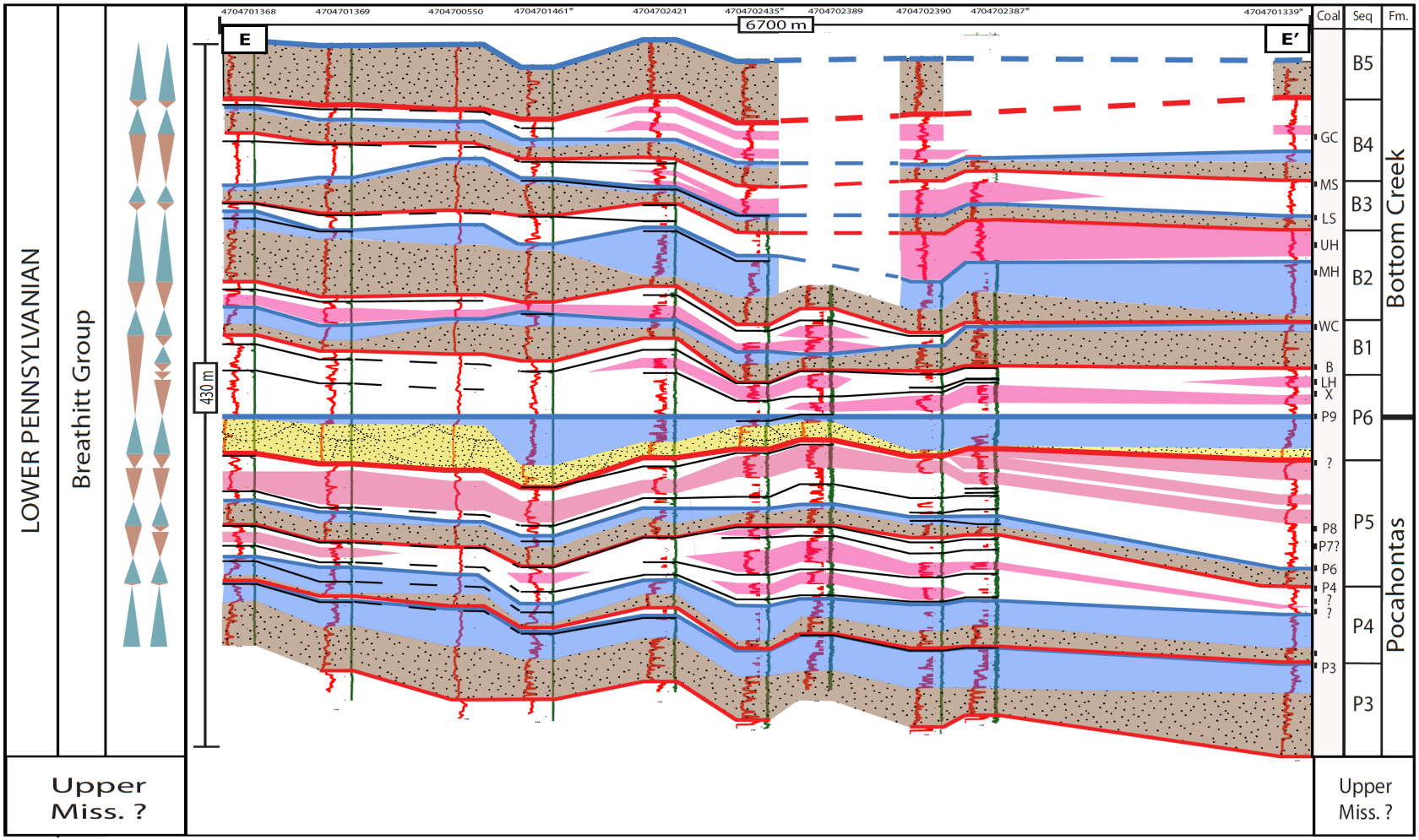

Figure 12. Dip-oriented (NW-SE) cross-section E-E′ (see Figure 6 for location). Displayed are minor discontinuities (thin red lines), major disontinuities (thick red lines), minor marine zones (thin blue lines), and major marine zones (thick blue lines). Sequences are bound by minor and major discontinuities. A complete sequence contains either quartzarenite (yellow) or sublitharenite (brown), followed by light blue fining-upward fluvial-estuarine facies and red coarsening-upward bay-fill deltaic facies. This cross-section displays 4 sequences in the Pocahontas formation and 5 sequences in the Bottom Creek Formation.

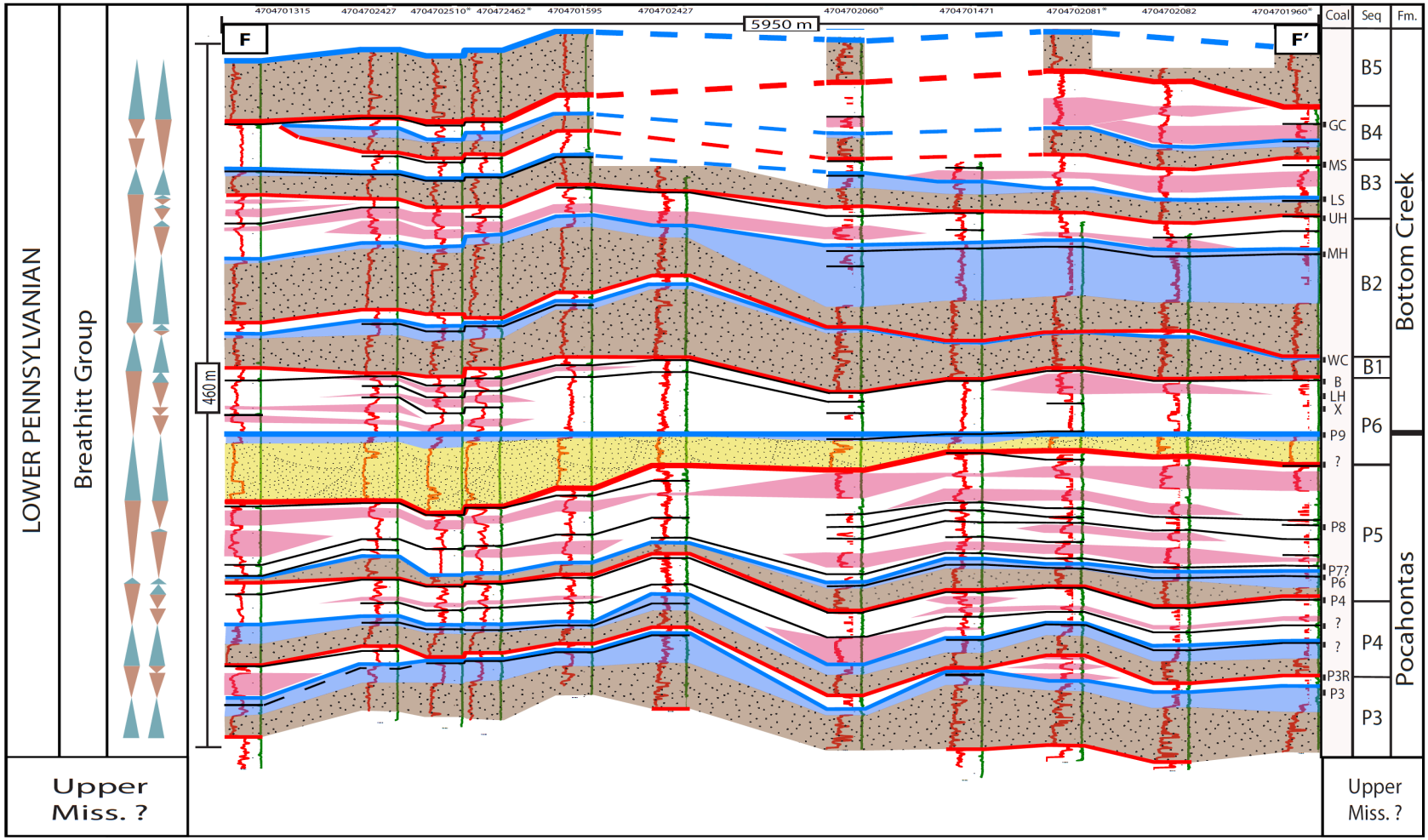

Figure 13. Dip-oriented (NW-SE) cross-section F-F' (see Figure 6 for location). Displayed are minor discontinuities (thin red lines), major disontinuities (thick red lines), minor marine zones (thin blue lines), and major marine zones (thick blue lines). Sequences are bound by minor and major discontinuities. A complete sequence contains either quartzarenite (yellow) or sublitharenite (brown), followed by light blue fining-upward fluvial-estuarine facies and red coarsening-upward bay-fill deltaic facies. This cross-section displays 4 sequences in the Pocahontas formation and 5 sequences in the Bottom Creek Formation.

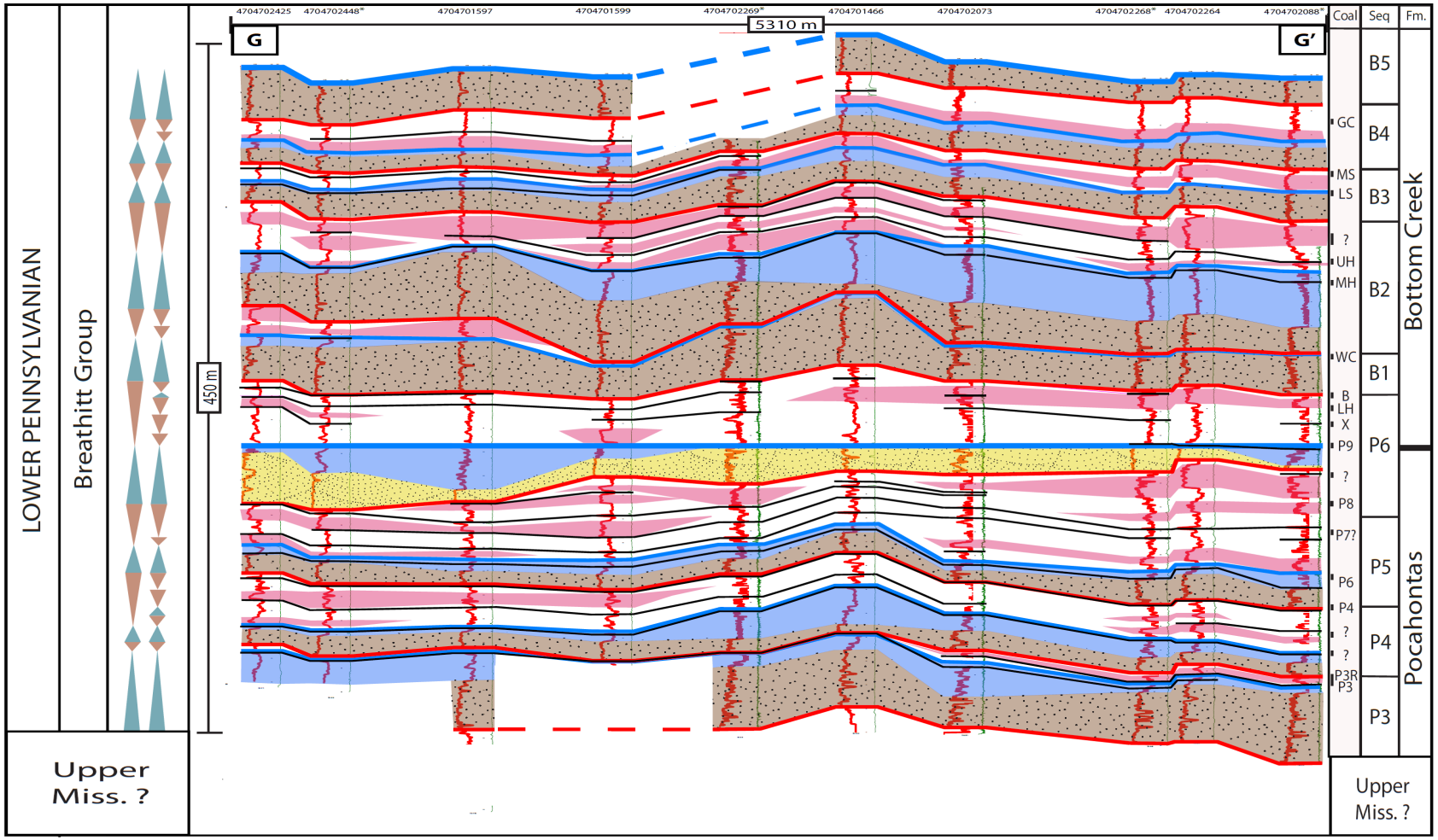

Figure 14. Dip-oriented (NW-SE) cross-section G-G' (see Figure 6 for location). Displayed are minor discontinuities (thin red lines), major disontinuities (thick red lines), minor marine zones (thin blue lines), and major marine zones (thick blue lines). Sequences are bound by minor and major discontinuities. A complete sequence contains either quartzarenite (yellow) or sublitharenite (brown), followed by light blue fining-upward fluvial-estuarine facies and red coarsening-upward bay-fill deltaic facies. This cross-section displays 4 sequences in the Pocahontas formation and 5 sequences in the Bottom Creek Formation.

5. DESCRIPTIONS

5.1. Facies and Gamma-Ray Responses

The facies descriptions are based on observations of mineralogy, grain-size, organic material, sedimentary structures, and biogenic structures from the outcrop in the study area. These descriptions are tied to their corresponding spectral gamma-ray log to identify gamma-ray log patterns for both facies and vertical facies transitions (**Fig. 5; Appendix A**). This study identifies eight facies subdivided into six distinct groups for lower Pennsylvanian strata: sandstones, heterolithic strata, mudstone, black shale, seat earth, and coal.

5.1.1. Sandstone facies

5.1.1.1. Quartzarenite

Quartzarenite facies of the Warren Point Formation at the I-77 outcrop locality are white to light-gray, fine to medium grained, well-sorted quartz-rich sandstones. Quartzarenite facies range from 20-30 meters thick and exhibit sheet-like geometry in outcrop (**Fig. 15A**).

Petrographic analysis of similar sandstones (Sewanee Formation equivalent) in southern West Virginia by Reed (2003) and Reed et al. (2005) classify these quartz-rich sandstones as quartzarenites (classification according to (Dott, 1964) consisting of 96% quartz (>95% monocrystalline), 3% lithics, and 1% feldspar.

The Warren Point Formation at the I-77 outcrop locality exhibits a sharp basal contact overlying black shale and coal facies, and a gradational upper contact into sandy and muddy heterolithics. Trough cross-bedding is common within the formation, present

in multi-storey, upward thinning packages ranging from 0.1 to 3 meters in thickness (**Fig. 15A**). Trough cross-beds give a west-southwest paleoflow direction (**Fig. 15B)**. Carbonaceous stringers, mudstone/coal rip-ups, and lithic casts are commonly found immediately above the basal contact, ranging from 0.3 to 0.6 meters in thickness (**Fig. 15C**).

Total gamma-ray values for quartzarenite facies in outcrop range from ~1170 to 1180 cps, lower than the immediately underlying sublitharenite (~1236 cps; **Appendix D**). This sharp contrast in gamma-ray values produces a well-defined sharp-based "box car" appearance (Walker, 1992). Subsurface gamma-ray logs show similar gamma-ray patterns for quartzarenites to those found in outcrop. The upper gradational contact of the quartzarenite facies in the subsurface is characterized by a gradual increase in gamma-ray values, as mineralogical immaturity and fines increase upward.

5.1.1.2. Sublitharenite

Sublitharenite facies are grayish orange to medium gray, fine- to medium-grained, moderately-sorted micaceous sandstones (**Fig. 16**). Sublitharenites are 3 to 20 meters thick and have lenticular and sheet-like geometry in outcrop.

Petrographic analysis of laterally equivalent sandstone bodies in Buchanan County, Virginia by Reed (2003) and Reed et al. (2005) classify these lithic sandstones as sublitharenites consisting of 77% quartz (monocrystalline), 15% lithics (metamorphic clasts) and 8% feldspar.

Sublitharenite facies at the Garwood, WV outcrop locality exhibit a sharp-basal contact (**Fig. 17A**) and gradational or abrupt upper contact. Upper and lower

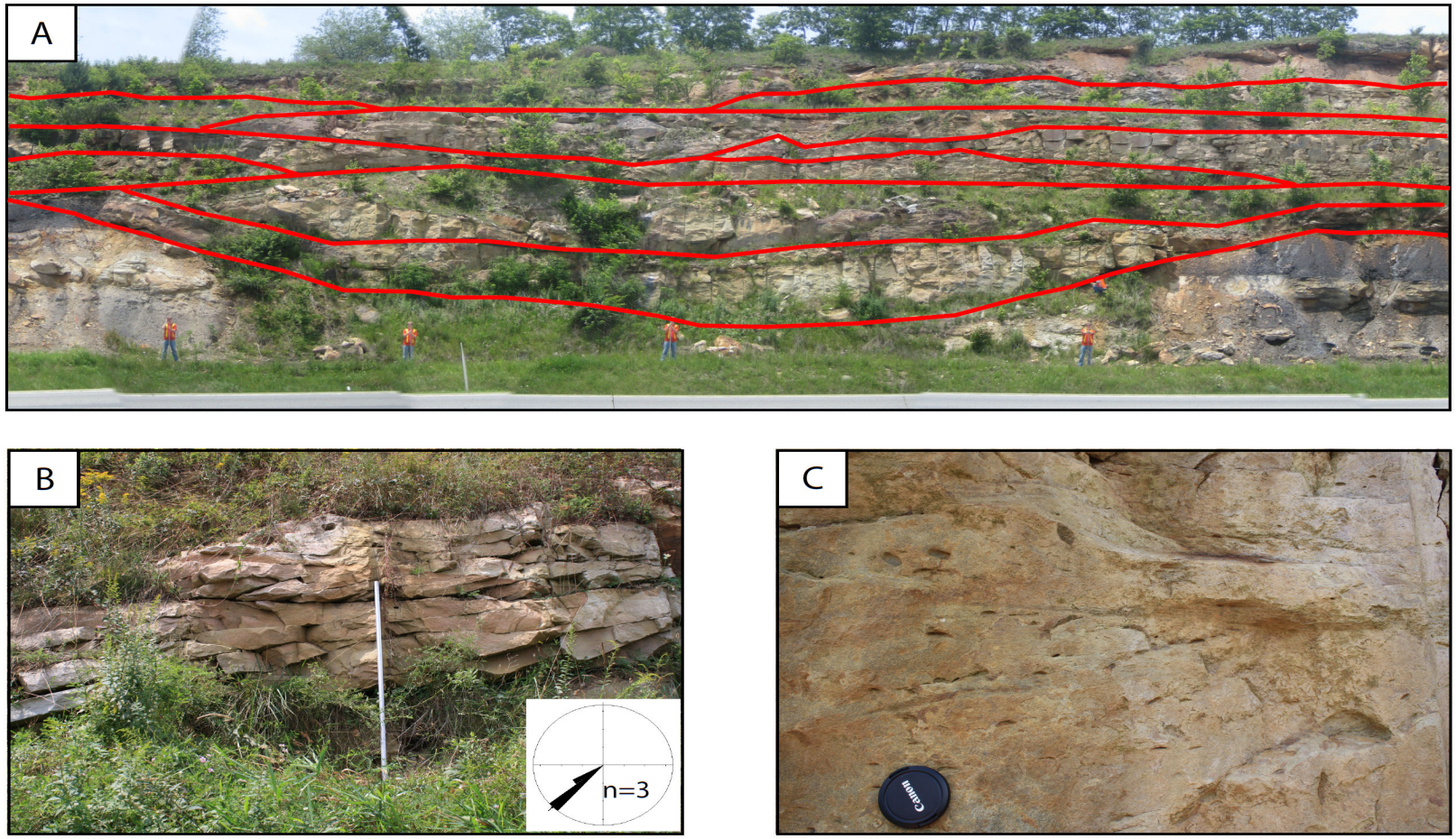

Figure 15. Quartzarenites of the Warren Point Formation, I-77. A) Photomosaic of multi-storey / multi-channel-fill complex (outlined in red; person = 5′ 8″ for scale). B) Longitudinal view of trough cross-bedding exhibiting southwest paleoflow (Jacob's staff = 5 ft for scale). C) Lithic casts within base of quartzarenite facies (camera lense cap = 72 mm diameter for scale).

Figure 16. Photomosaic of multi-storey / multi-channel fill complex (outlined in red) of Pocahontas No. 2 sublitharenite, I-77, WV. Note large scale trough cross-bedding (person = 5′ 8″ for scale).

bounding lithologies are generally sandy and muddy heterolithics. Carbonaceous stringers, mudstone/coal rip-up clasts, and (rarely) woody plant debris overlie the basal contact, ranging from 0.3 to 0.6 meters in thickness (**Fig. 17B**). Trough cross-bedding is the dominant sedimentary structure within sublitharenite sandstone bodies, present in multi-storey, upward thinning packages ranging form 0.3 to 3 meters in thickness (**Fig. 17C**). Rare, large-scale planar cross-bedding (2-3 m in thickness) is developed locally and commonly contains overlying mud drapes. Centimeter-scale laminations infrequently occur near the top of sublitharenite sandstone bodies (**Fig. 17D**). Massive, non-descript intervals are also present, ranging from 8 to 10 meters in thickness. Cross-beds give a west-northwest paleoflow direction (**Fig. 5; Appendix A**).

Total gamma-ray values for sublitharenite facies in outcrop range from ~1200 to 1260 cps, commonly lower than underlying lithologies. Sublitharenites have slightly higher gamma-ray values than quartzarenites, but exhibit a similar, "box car" appearance with serrated edges. Subsurface gamma-ray logs show a similar gamma-ray response for sublitharenites to those found in outcrop. Where gradational, the upper contact of the sublitharenite facies in the subsurface is characterized by a gradual increase in gamma-ray values similar to that of the quartzarenite facies.

5.1.2. Heterolithic facies

Heterolithic is a term used to describe strata consisting of interlaminated sandstone, siltstone, and mudstone (Walker, 1992). Sandy heterolithic strata are

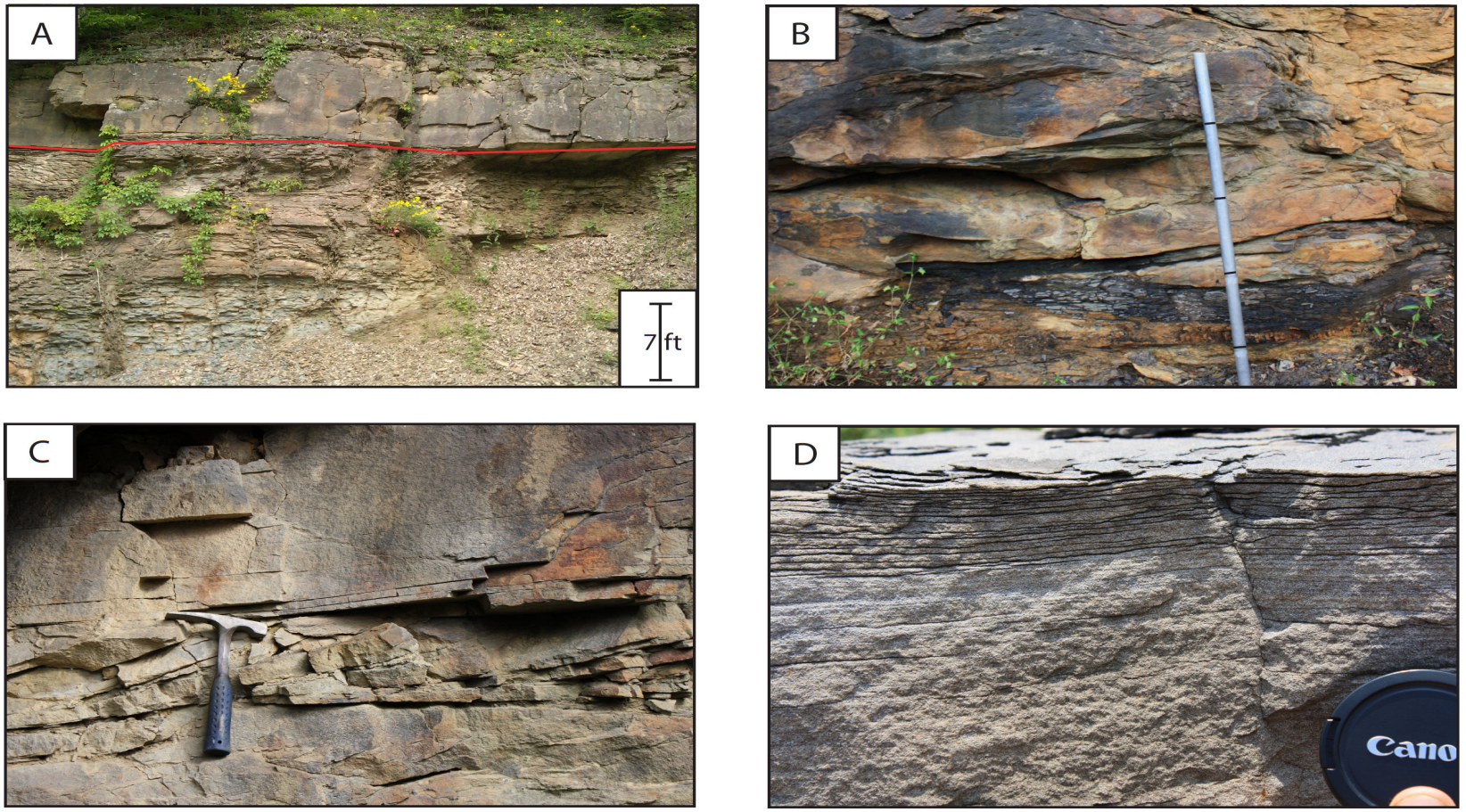

Figure 17. Sublitharenite facies. A) Sharp basal-contact (outlined in red) of Pocahontas No.1 sublitharenite body overlying muddy heterolithic strata, Garwood, WV (note scale). B) Carbonaceous stringers and coal rip-up clasts overlying the basal contact of the sublitharenite Warren Point Formation, Garwood, WV (Jacobs staff marked with 1 foot intervals for scale). C) Trough cross-bedding in the Pocahontas No.2 sublitharenite body , Garwood, WV (rock hammer = 2 ft for scale). D) Parallel laminations at top of Pocahontas No.1 sublitharenite body, I-77, WV (camera lense cover = 77 mm for scale).

comprised of greater than 50% sandstone, with lesser amounts of siltstone and mudstone, whereas muddy heterolithic strata are comprised of greater than 50% mudstone, with lesser amounts of sandstone and siltstone. Heterolithic facies occur intercalated within ~6-30 m thick fine-grained intervals of mudstone, carbonaceous mudstone, and coal. Heterolithic facies commonly have spheroidal weathering in outcrop (**Fig. 18A**).

5.1.2.1. Sandy heterolithic

Sandy heterolithic facies consist of light- to medium-gray, fine-grained, interlaminated micaceous sandstones and mudstones and are 0.3 to 2 meters thick in outcrop. Basal and upper contacts of sandy heterolithic facies are generally gradational. Bounding lithologies vary from sublitharenites to muddy heterolithics, based on the position of this facies within the stratigraphic column (**Fig. 5; Appendix A)**. Sandy heterolithics commonly have flaser bedding, with individual cross-bed sets ranging from 1 to 3 cm thick.

Total gamma-ray values for sandy heterolithic facies in outcrop range from ~1250 to 1280 cps. This wide range in gamma-ray values is attributed to imprecision of the GRS system coupled with the thinnessof the facies. Because the range of total gamma-ray values overlaps with that of sublitharenites, it is difficult to identify the extent of sandy heterolithic facies in the subsurface, especially at the sublitharenite to sandy heterolithic transition. Sandy heterolithic facies are loosely identified in the subsurface as having “moderate” gamma-ray values due to a higher sand to mud ratio.

5.1.2.2. Muddy heterolithic

Muddy heterolithic facies are dark- to very dark-gray mudstone intervals with light- to medium-gray, lenticular, siltstone and fine-grained sandstone lenses (**Fig. 18B, 18C**). Muddy heterolithic facies are 0.3 to 8 meters thick in outcrop.

Muddy heterolithic facies generally have a gradational basal contact and abrupt upper contact. Bounding lithologies range from sublitharenites to sandy heterolithics to mudstones. Muddy heterolithic facies commonly are lenticular bedded, with individual cross-laminated lenses ~1 cm thick (**Fig. 18B**). Many muddy heterolithic units contain plant fossil-rich and rooted mudstone intervals (**Fig. 18C**).

Total gamma-ray values for muddy heterolithic facies range from ~1245 to 1300 cps**.** As with the sandy heterolithic facies, the wide range of total gamma-ray values for muddy heterolithic facies is attributed to imprecision in the GRS system as well as the thin nature of the facies. This wide range in gamma-ray values makes identification of muddy heterolithic facies extremely difficult in the subsurface. Muddy heterolithic facies are loosely identified in the subsurface as having moderate to moderately-high gamma-ray values due to a relatively high mud to sand ratio.

5.1.3. Mudstone facies

Mudstone facies are dark-gray to very dark-gray, very fine-grained units from 0.3 to 3 meters thick in outcrop. Mudstone facies are commonly intercalated with muddy heterolithic facies. Small-scale laminations are present throughout and they commonly contain abundant plant fossils in the Garwood section, including *Neuropteris pocahontas*,

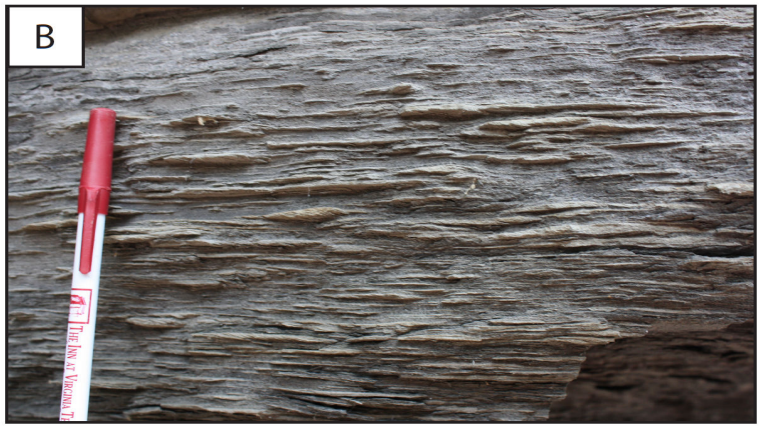

Figure 18. Heterolithic facies. A) Spheroidal weathering pattern in outcrop common in muddy and sandy heterolithic facies (field book = 19 mm for scale). B) Centimeter scale lenticular-bedding in muddy heterolithic facies (pen cap ~ 2" for scale). C) Differential weathering in muddy heterolithic facies related to varying amounts of sand lenses within the facies (Jacobs staff marked with 1 foot intervals for scale). The greater the sand content, the more resistant to weathering.

Lepidodendron dichotomum, Mariopteris pottsvillea, Alethopteris evansi, A. davreuxi, Mariopteris pottsvillea, M. eremopteroides, Aneimites pottsvillensis, Sphenopteris preslesensis, and others (**Fig. 19)** (Englund et al., 1979).

Total gamma-ray values of mudstone facies in outcrop range from ~1270 to 1300 cps. Identification of mudstone facies in the subsurface poses similar challenges to that of the heterolithic facies described above. Mudstone facies are loosely identified in the subsurface as having high gamma-ray values due to their high percentage of mud.

5.1.4. Black shale facies

Black shale facies are dark-gray to black and range from 0.2 to 1.5 meters thick in outcrop (**Fig. 20A**). They contain similar plant debris and fossils as mudstone facies. Black shales are typically closely associated with coal-beds, and commonly contain stigmarian rootlets where overlain by a coal.

Total gamma-ray values of black shale facies in outcrop range from ~1250 to 1300 cps. This wide range in gamma-ray values poses similar problems to identification in the subsurface as the heterolithic and mudstone facies. Where significantly thick (1.5+ meters), black shales are easily identified in the subsurface as having gamma ray values over 1300 cps, allowing for correlation of this facies between wells.

5.1.5. Seat earth facies

The seat earths are mudstone paleosols that contain coal organic matter and thus are histosols (Mack et al., 1993). Seat earth facies range from 0.1 to 0.9 meters thick in outcrop. Two horizons within the paleosols are evident in seat earth facies, an orange to

Figure 19. Plant fossils in mudstone / muddy heterolithic facies above the Pocahontas No.3 coal, I,77, WV (dime ~ 2 mm in diameter for scale).

brown B horizon containing plant debris and stigmarian rootlets, overlain by a light gray, non-descript A horizon. The seat earth is commonly underlain by black shale facies, and overlain by a coal O horizon (**Fig. 20B)**.

Total gamma-ray values of seat earth facies in outcrop range from ~1260 to 1300 cps. Seat earth facies generally exhibit similar gamma-ray values to bounding lithologies due to the thinness of the facies. Recognition of this facies in the subsurface is unfeasible.

5.1.6. Coal facies

Southern West Virginia coal is ranked as high-volatile bituminous, with an average sulfur content of 1.1% and less than 10% ash (Administration, 1994). High quality Lower and Middle Pennsylvanian coals have become an emerging resource for coal-bed methane, containing an estimated 3.07 Tft^3 of recoverable coal-bed methane gas in the Central Appalachian Basin (Ryder, 1995). The Bradshaw CBM field was developed to target methane contained in lower Pennsylvanian coals. These coals include the Pocahontas #3, Pocahontas #4, Lower Horsepen, War Creek, Beckley, Lower Seaboard Raven, and Jawbone (Ruppert and Rice, 2000).

Coal thickness was determined by direct measurement in outcrop coupled with subsurface bulk density log data. Coal thickness is calculated by measuring the area under the bulk density curve that falls below 1 g/cm^3 (Denning, 2008). Coals in the study area range from 1 – 60 inches in thickness. Coals are generally found stratigraphically below sharp-based quartzarenite and sublitharenites bodies, and interbedded with fine-grained mudstone and heterolithic facies (**Fig. 20C**).

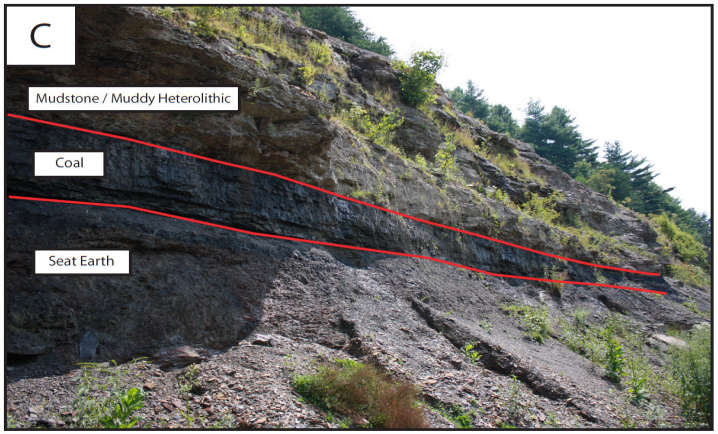

Figure 20. Black shale, seat earth, and coal facies, I-77. WV A) Black shale with scintillometer probe for scale. B) Seat earth below Pocahontas No.3 coal. Note paleosol horizons (orangish-red B horizon, grey A horizon) Jacobs staff marked with 1 foot intervals for scale. C) Pocahontas No.3 coal (outlined in red; coal ~ 4 feet thick for scale).

Underlying mudstone and black shales are generally heavily rooted and contain abundant plant debris.

Total gamma-ray values for coal in outcrop range from ~1220 to 1260 cps, similar to bounding lithologies. In the subsurface, coal-beds have low gamma-ray values similar to that of quartzarenites, making determinations of coal thickness based only on gamma-ray difficult. Coals are most easily identified with bulk density logs, generally having values below 2 g/cm^3.

5.2. Facies Successions

A comparison of gamma-ray values of the above facies with the stratigraphic log (**Fig. 5; Appendix A)**, reveal patterns that are both predictable and vertically repetitive (Bodek, 2006). Bodek (2006) and Denning (2008) provide summaries of diagnostic gamma-ray signatures that correspond to particular lithofacies or vertical successions of lithofacies.

5.2.1. Upward-fining successions

Quartzarenite and sublitharenite sandstone bodies in outcrop become finer-grained upwards, with a gradational transition from medium-grained sandstone facies at the base to fine-grained, sandy heterolithic facies at the top. This "dirtying" upward results in increasingly higher gamma-ray values toward the top of the sandstone. Upward-fining continues through a gradational facies change from sandy heterolithic to muddy heterolithic to mudstone, resulting in high gamma-ray values. The upward-fining succession is commonly capped by a moderately thick mudstone intercalated with black

shale and coal, producing a high gamma-ray spike identifiable in subsurface datasets. The overall gamma-ray trend is represented by a large rise in gamma-ray values which steadily increases toward the top of the interval and culminates in a "hot" gamma-ray spike.

5.2.2. Upward-coarsening successions

Coarsening-upward facies successions are characterized by a gradational transition from mudstone to sandstone facies. The succession progresses from muddy/black shale facies to heterolithic facies to fine-grained sublitharenite facies. As facies become progressively coarser, gamma-ray values gradually decrease. Thinner upward-coarsening to upward-fining intervals may be present within the overall upward-coarsening succession. The higher frequency upward-coarsening succession begins at the base of a mudstone that overlies a laterally persistent coal bed, and coarsens upward to mixed heterolithic facies. The number of higher frequency upward-coarsening to upward-fining successions within the overall upward-coarsening succession is variable.

5.3. Architectural Elements

An architectural element is "a morphological subdivision of a particular depositional system characterized by a distinctive assemblage of facies, facies geometries, and depositional processes" (Walker, 1992). Architectural elements are identified in outcrop (see *Descriptions*), and are translated to the subsurface through identification of distinct gamma-ray values and patterns of unique facies. Architectural elements for facies observed in outcrop include sheet-like sandstone, lenticular sandstone,

and mudstone elements. Difficulty in identifying sandy and muddy heterolithic facies in the subsurface prompts the use of predictable gamma-ray patterns for upward-fining and upward-coarsening facies successions in their place.

5.3.1. Sheet-like sandstone elements

Sheet-like sandstone elements are comprised of quartzarenite and sublitharenite sandstone bodies in the study area. In cross-section, sheet-like sandstone elements appear tabular and range from 12-30 m in thickness (**Figs. 8-14;** Sequence P6). Sheet-like sandstone bodies are sharp based, characterized by fine- to medium-grained sandstones. Rip-up clasts of mudstone and coal are commonly found above the basal contact. Sheet-like sandstone elements become finer grained upward, grading into overlying heterolithic facies.

5.3.2. Lenticular sandstone elements

Lenticular sandstone elements are comprised of thin (1-3 m) and thick (12-30 m) sublitharenite and minor sandstone bodies within the study area (**Figs. 8-14**). Thick lenticular sandstone elements are characterized by sharp-based sandstone lenses comprised of medium-grained micaceous sandstones that pinch out laterally. Where lenses pinch out, they are replaced by upward-coarsening facies successions (**Fig. 13;** Sequence B4). Thick lenticular sandstone elements grade upward to heterolithic facies. Thin lenticular sandstone elements are characterized by fine-grained micaceous sandstones. These elements generally lack sedimentary structures. Thin lenticular sandstone elements commonly grade into bounding lithologies.

5.3.3. Upward-fining elements

Upward-fining elements are characterized by the gradational transition from sandy and muddy heterolithic facies to mudstone and black shale facies. This transition is defined by a steady increase in gamma-ray values. Upward-fining elements gradationally overlie both sheet-like and lenticular sandstone elements, and are commonly capped by a coal (**Figs. 8-14**). Where lenticular sandstone elements pinch out, upward-fining elements directly overlie upward-coarsening elements (**Figs. 13;** Sequence B4). Upward fining elements, where present, range from 3-15 m thick.

5.3.4. Mudstone-dominated elements

Mudstone-dominated elements are comprised of either all mudstone or alternating intervals of mudstone and muddy heterolithic facies (**Figs. 8-14**). These elements range from 1.5-5 m in thickness. Mudstone-dominated elements generally overlie coal beds capping upward-fining elements, and are capped by sandy-heterolithic facies.

5.3.5. Upward-coarsening elements

Upward-coarsening elements are comprised of 6-60 m thick tabular intervals of coal, overlain by black shale, mudstone, heterolithic, and sandstone facies (**Figs. 8-14**). Upward-coarsening elements overlie mudstone-dominated elements, and are sharply truncated by overlying sheet-like and lenticular sandstone elements. Higher frequency upward-coarsening to upward fining intervals are present within the overall upward-coarsening succession, and range from 3-15 m in thickness.

5.4. Bounding Discontinuities

Architectural elements are bound by regionally extensive discontinuities, both erosional (unconformable) and depositional (condensed) (Walker, 1992). Major and minor erosional discontinuities have been identified in lower Pennsylvanian strata of the central Appalachian basin (Aitken and Flint, 1994; Bodek, 2006; Denning, 2008; Korus et al., 2008; Korus, 2002). Both erosional and depositional discontinuities can be traced laterally within the study area in both strike and dip directions (**Figs. 7-14)**.

Major erosional discontinuities (**Figs. 8-14;** Sequences P6 and B5**)** have relatively thin intervals of fine-grained facies preserved beneath the erosional contact and, in some cases, complete erosional removal of fine-grained facies results in the amalgamation of sheet-like sandstone elements (Bodek, 2006; Denning, 2008).

Minor erosional discontinuities (**Figs. 8-14;** Sequences P3-P5, B1-B4**)** have relatively thick intervals of fine-grained facies preserved beneath the erosional contact. Minor erosional discontinuities are commonly found at the bases of thick sheet-like and lenticular sublitharenite sandstone bodies. Where lenticular sandstone elements pinch out laterally, the minor discontinuity is placed at the top of the equivalent upward-coarsening elements (**Figs. 13;** Sequence B4). Aitken and Flint (1995) found the position of regionally extensive coals to correlate with minor erosional discontinuities in upward-coarsening successions.

Major and minor depositional discontinuities (marine zones) have also been identified in the study area based on their stratigraphic position in cross-section. Major marine zones occur as thick (9-27 m) intervals of coal, black shale, mudstone, and

heterolithic strata overlying sheet-like quartzarenite sandstone bodies. In this study, one major marine zone is identified overlying the Warren Point formation, corresponding to the Dark Ridge Member marine zone demarcating the boundary between the Pocahontas and Bottom Creek formations. Regionally extensive coals associated with the Dark Ridge member include the Pocahontas #7, 8, 9, and X seams. Minor marine zones occur as relatively thin (0.3-3 m) intervals of mudstone, black shale, and coal located at the top of upward-fining successions overlying minor erosional discontinuities. Minor marine zones represent the sole source of depositional discontinuity within the Pocahontas Formation.

6. INTERPRETATION

6.1. Fluvial Sandstone Elements

6.1.1. Sheet-like quartzarenite elements

Sedimentary structures within limited exposure of sheet-like quartzarenites of the Warren Point Formation at I-77 are consistent with a fluvial depositional model (cf. (Archer and Greb, 1995; Beuthin, 1994; Bodek, 2006; Denning, 2008; Rice and Schwietering, 1988). Carbonaceous stringers and mudstone/coal rip-ups immediately above the basal contact are interpreted as channel lag deposits (cf. (Bodek, 2006; Denning, 2008; Miall, 1985). Trough cross-bed sets give a unimodal west-southwest paleoflow direction (**Fig. 15B**) and are interpreted as the product of three-dimensional dunes migrating down a bedload-dominated channel. Paleoflow direction is along the axis of the Alleghanian foreland basin. The multi-storey architecture of trough cross-bed sets is characteristic of multi-channel braided river deposits. Sheet-like quartzarenites of

the Warren Point formation are thus interpreted as major incised valley fills deposited by bed-load dominated braided rivers along the axis of the Alleghanian foreland basin via downstream accretion. This agrees with the interpreted depositional environments of equivalent sandstones in Kentucky and Virginia, attributed to downstream accretion of bedforms, macroforms, and channel fill elements during high and waning flow stages (Bodek, 2006; Denning, 2008; Wizevich, 1992). Braided-rivers depositing sheet-like quartzarenites were sourced by the cratonic Archean Superior Province to the north (Archer and Greb, 1995; Bodek, 2006; Denning, 2008; Greb and Chesnut, 1996; Korus, 2002; Rice, 1985).

6.1.2. Sheet-like sublitharenite elements

Sheet-like sublitharenites of the Pocahontas Formation contain a characteristic vertical succession of sublithofacies diagnostic of fluvial deposition. Basal lags of wood debris, plant remains, and calcareous mud / coal stringers developed along channel bases and are interpreted as channel lag deposits (cf. (Bodek, 2006; Denning, 2008; Miall, 1985). Trough cross-bed sets are interpreted as the product of three-dimensional dunes migrating down a bedload dominated channel. Paleoflow direction indicates west-northwest paleoflow (**Fig. 5**), transverse to paleoflow of sheet-like quartzarenites of the Warren Point Formation. The multi-storey architecture of trough cross-bed sets is characteristic of multi-channel braided river deposits. Minor, large-scale planar cross-bed sets also exhibit west-northwest paleoflow (**Fig. 5**), and are interpreted as the product of two-dimensional dunes migrating downstream. Parallel laminations found interspersed within sheet-like sublitharenite elements are produced by planar bed flow

which can occur in both upper and lower flow regimes, and are commonly found distributed throughout fluvial-bar deposits (Allen, 1993). Sheet-like sublitharenite elements of the Pocahontas Formation are thus interpreted as minor incised valley fills deposited by bedload dominated braided rivers draining the low-grade metamorphic terrain of the Alleghanian orogen to the southeast (Bodek, 2006; Denning, 2008; Korus, 2002).

6.1.3. Lenticular sublitharenite elements

Lenticular sandstone elements of the Pocahontas Formation are comprised of thin (1-3 m; **Figs. 8-14;** minor sandstone bodies**)** and thick (12-30 m; **Fig. 13;** Sequence B4) sublitharenite sandstone bodies within the study area. Thick lenticular sublitharenite elements share the sedimentary characteristics of sheet-like sublitharenite elements above, and are similarly interpreted as minor incised valley fills deposited by bedload dominated braided rivers draining the low-grade metamorphic terrain of the Alleghanian orogen to the southeast (Bodek, 2006; Denning, 2008; Korus, 2002)

Thin lenticular sublitharenite bodies are intercalated with sandy and muddy heterolithic facies. Whereas thin lenticular sublitharenites retain a sharp basal contact and cross-bedding similar to thick lenticular sublitharenites, they commonly lack mudstone and coal rip-up clasts above the basal contact. Due to their stratigraphic position and relative interval thickness, thin lenticular sandstone elements are interpreted as being deposits of small crevasse channels (in fluvial settings) or delta distributary channels (in estuarine settings) (see *Upward-Coarsening Elements*).

6.2. Upward-Fining Elements

Upward-fining elements cap quartzarenite and sublitharenite sandstone bodies, indicating waning flow conditions related to a decrease in stream gradient associated with base-level rise (Bodek, 2006; Denning, 2008). Continued base-level rise resulted in the formation of backswamp-floodplain complexes (in fluvial settings) and estuaries (in mixed fluvial / marine settings) due to flooding of incised valleys.

Upward-fining elements of the Pocahontas Formation are characterized by sandy and muddy heterolithics, laminated mudstones, black shales, and coal. Allen (1993) interpreted a levee-overbank and backswamp-floodplain environment for these facies at the Garwood, WV outcrop locality. This study forgoes Bodek's (2006) and Denning's (2008) estuarine interpretation for upward-fining elements in the Pocahontas Formation in favor of Allen's (1993) depositional interpretation due to the lack of tidal indicators and abundance of well-preserved plant debris within upward-fining elements in the Pocahontas Formation. Heterolithic strata overlying braided river sublitharenites are interpreted as levee-overbank deposits. Flaser and lenticular bedding within heterolithic strata are indicative of alternating bedload and suspension deposition common in levee-overbank deposits (Reineck and Wunderlich, 1968). Continued flooding resulted in the formation of a broad backswamp-floodplain environment, with water depths ideal for the accumulation of peat that would eventually develop into laterally extensive coals. As the rate of flooding increased, the peat mires were drowned out and thick-laminated mudstones and black shales were deposited in backswamp complexes by slow suspension deposition. Freshwater fossils have been reported in the roof shale of the Pocahontas No.

6 coal bed (Hennen and Gawthrop, 1915; Krebs, 1916; Price, 1916; Reger, 1926), further supporting a backswamp-floodplain depositional environment (Allen, 1993).

While a majority of the upward-fining elements in the Pocahontas Formation are characteristic of fluvial point bar floodplain deposits, a transition from fluvial to estuarine conditions is apparent late in the deposition of the Pocahontas Formation. Reports of marine fauna occurring in the roof mudstone of the Pocahontas No. 8 coal-bed (Henry and Gordon Jr, 1979) indicate that marine to brackish conditions existed following deposition of the Pocahontas No. 8 coal (Allen, 1993). This suggests that the depositional environment for the Pocahontas Formation underwent a transition from an entirely continental upper-delta plain to an estuarine-marine-influenced lower-delta plain late in its depositional history (Allen, 1993). Bodek (2006) and Denning (2008) document tidal influences in upward-fining elements within the Bottom Creek Formation, suggesting that a lower-delta plain depositional environment persisted throughout the lower Pennsylvanian after deposition of the Pocahontas No. 8 coal.

6.3. Mudstone-Dominated Elements

Mudstone and black shale elements directly overlie upward-fining successions, recording maximum base-level rise and drowning of the peat mire by clastics (cf. Shanley and McCabe, 1994). Multiple mudstone and black shale elements can be found in overall upward-fining elements, suggesting periods of minor base level fluctuations and peat mire drowning events (Denning, 2008).

6.4. Upward-Coarsening Elements

Upward-coarsening elements are interpreted as progradation of crevasse-splay complexes (in fluvial settings; Allen, 1993) and progradation of bayhead deltas toward the northwest Appalachian Seaway during late stages of base level rise through early base level fall (in mixed fluvial / marine setting; Korus, 2008; Greb and Martino, 2005; Bodek, 2006; Denning, 2008).

Overall, upward-coarsening elements of the Pocahontas Formation are comprised of repetitively stacked upward-coarsening to upward-fining intervals of muddy heterolithic, sandy heterolithic, and thin lenticular sublitharenite facies. Upward-coarsening successions of muddy heterolithics to sandy heterolithics are interpreted as progradation of crevasse-splay and bay-head delta complexes across backswamp-floodplain environments (Allen, 1993). Thin lenticular sandstone elements that cap upward-coarsening packages correspond to distal-bar, mouth-bar, and channel deposits (**Figures 7-14)** (Bhattacharya et al., 1992; Coleman and Wright, 1975; O'Mara and Turner, 1999; Reading and Collinson, 1996). Upward-fining intervals within overall upward-coarsening elements are interpreted as crevasse splay or distributary channel deposits. These channels can develop into an estuary, resulting in upward-fining intervals of fill (Bhattacharya et al., 1992). Deltaic deposits within the study area are interpreted to be those of river-dominated delta lobes, similar to those of the Cretaceous Dunvegan Formation (Bhattacharya et al., 1992).

Coals capping upward-fining intervals in overall upward-coarsening elements represent peat mire development on top of abandoned delta lobes (cf. (Coleman, 1976) . Peat mire development in general is thought to be controlled by localized transgressions

driven by dewatering and compaction-induced subsidence (Bhattacharya et al., 1992; Coleman, 1976).

6.5. Overview of Sequence Stratigraphic Concepts

Sequence stratigraphy is the study of chronologically significant frameworks of genetically related, unconformity-bound intervals of sedimentary strata (Van Wagoner et al., 1990; Van Wagoner et al., 1988). The basic building blocks of depositional sequence stratigraphy are 'sequences,' relatively conformable, genetically related strata bound by unconformities or their correlative conformities (Mitchum, 1977). Sequences consist of stacked parasequences (composed of lamina, laminasets, beds, and bedsets) bound by flooding surfaces (Van Wagoner et al., 1988). Internal packaging of progressively thicker stratal units representing increasing amounts of time defines a chronostratigraphic hierarchy (Mitchum and Van Wagoner, 1991; Van Wagoner et al., 1990). Lower-order (shorter duration) sequences are found to stack within higher-order (longer duration) sequences in a repetitive and predictable fashion. Predictable facies stacking patterns, sediment body geometry, and position along depositional dip enable interpretation of depositional controls on the system. Depositional controls, including eustasy, tectonism, climate, and sediment supply, dictate base level variability. Thus, base level is a primary control on sequence development.

In terrestrial settings, base level represents the lower limit of subaerial erosion, or sea-level (Powell et al., 1875). The direction and magnitude of relative sea-level changes is a result of the combined effects of eustasy and tectonic uplift/subsidence (Holz et al., 2002; Posamentier et al., 1988). This change in sea level is referred to as relative sea

level change, and can magnify, retard, or counteract the direction of global eustatic change. Direction and magnitude of relative sea level change exercises the greatest control on hierarchical sequence development and internal stacking patterns. Thus, sequence stacking patterns can be related to both the rate and direction of relative sea level change. Packages of unique stacking patterns are referred to as one of three systems tracts: lowstand systems tract (LST), transgressive systems tract (TST), and highstand systems tract (HST) (Posamentier et al., 1988; Van Wagoner et al., 1990; Van Wagoner et al., 1988). These systems tracts occur as a response to relative sea level fall, rapid rise, and peak, respectively.

Periods of sea level change can be linked to the development of systems tracts and bounding discontinuities, or sequence boundaries, within individual sequences. Sequence boundaries are formed during the maximum rate of sea level fall. Van Wagoner et al. (1988) recognize two types of sequence boundaries. Type 1 sequence boundaries are formed when the rate of sea level fall is greater than the rate of basin subsidence, creating a relative sea level fall at the depositional-shoreline break. Van Wagoner et al. (1988) attribute the resulting subaerial erosion to stream rejuvenation, a basinward shift in facies, a downward shift in coastal onlap, and onlap of overlying strata. Type II sequence boundaries are formed when the rate of sea level fall is less than the rate of basin subsidence, resulting in no relative sea level change at the depositional-shoreline break. While Type II sequence boundaries also exhibit subaerial erosion and a downward shift in coastal onlap similar to Type I sequence boundaries, they lack subaerial erosion due to stream rejuvenation and a basinward shift in facies (Van Wagoner et al., 1988).

Lowstand systems tracts are found only above Type I sequence boundaries. LSTs are formed during late stages of relative sea level fall through incipient sea level rise, characterized by aggradation as sediments being delivered to the basin via fluvial systems onlap the basal sequence boundary in a landward direction (Shanley and McCabe, 1994). A transgressive surface separating aggradationally stacked lowstand deposits from retrogradationally stacked transgressive deposits (Van Wagoner et al., 1988) marks the top of the lowstand systems tract, but is often difficult to identify due to the lack of a vertical facies change (Reading and Collinson, 1996; Walker and James, 1992).

The transgressive systems tract develops as continued sea level rise drowns incised valleys to form estuaries. The maximum flooding surface, represented by a highly radioactive black shale in marine strata (Galloway, 1989) and the onset of marine processes in alluvial strata (Shanley and McCabe, 1994), marks the upper limit of retrogradational transgressive deposits.

The highstand systems tract develops as relative sea level continues to rise through early sea level fall. HSTs are characterized by a period of aggradation followed by progradation of upward-coarsening deposits overlying retrogradationally stacked transgressive deposits (Van Wagoner et al., 1988). HSTs consist of broadly upward-coarsening successions of prograding deltaic facies. The highstand systems tract terminates as sea level drops to form another sequence boundary.

6.6. Sequence Stratigraphic Interpretation of Lower Pennsylvanian Strata

A genetic sequence stratigraphic framework based on maximum flooding surfaces identified three major marine zones in the lower Pennsylvanian Breathitt Group, dividing

it into three formations of approximately 2.5 m.y. duration (Chesnut, 1994; Greb et al., 2004) corresponding with a longer-term Milankovitch eccentricity signal (Matthews and Frohlich, 2002). These include the Pocahontas, Bottom Creek, and Alvy Creek formations which are capped by the Dark Ridge, Hensley, and Dave Branch shale members, respectively (Denning, 2008). Bodek (2006) has suggested duration of ~6.4 m.y. for the lower Pennsylvanian.

The bases of the sheet-like quartzarenite Warren Point (**Figs. 7-14; Sequence P6**) and sublitharenite Sewanee equivalent formations (**Figs. 7-14; Sequence B5**) are interpreted as 3rd-order sequence boundaries, lying stratigraphically beneath 3rd-order marine flooding surfaces of the Dark Ridge and Hensley shale members, respectively. Third-order sheet-like quartzarenites are interpreted as major incised valley fills, while sheet-like sublitharenites are interpreted as minor incised valley fills (see *Interpretations)*.

Minor discontinuities are associated with the base of both sheet-like and lenticular sublitharenites, reflecting incision into underlying lithologies. These minor discontinuities are considered to represent sequence boundaries, as the erosional discontinuity is regionally extensive. Minor marine flooding zones are located stratigraphically above minor sequence boundaries. In the cross-sections (**Figs. 7-14**), four minor sequences are present within the Pocahontas Formation. Assuming a 2.5 m.y. duration for the Pocahontas Formation, minor sequences have duration of ~600 k.y. Inferred duration of minor sequences of the Pocahontas Formation in the Bradshaw CBM field are comparable in duration to the minor sequence recognized by Denning (2008) for the lower Pennsylvanian Pocahontas, Bottom Creek, and Alvy Creek Formations.

Denning (2008) rejected his minor sequence duration estimate in favor of Bodek's (2006) 400 k.y minor sequence duration (attributed to Milankovitch long-term eccentricity cycles), arguing that fewer sequences developed in that particular locale of the Pocahontas basin. A comparison of the gamma-ray signatures of Pocahontas sublitharenite facies in outcrop at Garwood, WV to those of the Bradshaw CBM field reveals that the basal sandstone body in the Bradshaw field is likely the sublitharenite facies at the base of the P3 sequence, implying preservation of additional early Pennsylvanian sequences at the more basinward Garwood location and a missing interval of earliest Pennsylvanian sequences at the Bradshaw CBM field. Assuming the P3 sequence is the basal sequence developed in the Bradshaw field, two sequences (P1 and P2) are missing, bringing the number of total minor sequences within the Pocahontas Formation to six, with a duration of 417 k.y. Minor sequences are thus interpreted as 4^{th}-order cycles bound by 4^{th}-order sequence boundaries.

Fourth-order minor marine flooding zones are developed stratigraphically above 4^{th}-order sequence boundaries. While 4^{th}-order minor marine flooding zones contain similar strata to that of 3^{rd}-order major marine flooding zones, they are commonly almost an order of magnitude thinner than their 3^{rd}-order counterparts (**ex. Figs. 7-14; Sequence P4**).

Third-order composite sequences are comprised of several 4^{th}-order sequences within the study area, sharing a common sequence boundary with the basal 4^{th}-order sequence (**Figs. 7-14; base of Sequences P6 and B5**). This hierarchy of sequences has been documented by numerous researchers in Pennsylvanian strata, including Chesnut

(1994), Korus (2002), Greb et al. (2004), Bodek (2006), Korus et al. (2008), and Denning (2008).

The lowstand systems tract (LST) is identified by a sharp erosionally based incised valley fill deposits and correlative interfluves (McCarthy and Plint, 1998). LSTs consist of cross-bedded quartzarenites and sublitharenites that fine-upward, capped by the transgressive surface. The transgressive surface is defined as the first appearance of tidally influenced sedimentation, and demarcates the lowstand systems tract from the transgressive systems tract (Reading and Collinson, 1996; Zaitlin et al., 1994). In this study, the transition from fluvial to estuarine facies is identified as a change from quartzarenite and sublitharenite facies to sandy and muddy heterolithic facies.

The transgressive systems tract is identified in this study as an upward-fining facies succession of sandy heterolithics, muddy heterolithics, mudstones, black shales, and coal. The upper contact of the TST is commonly demarcated by black shales immediately overlying TST coals. These black shales formed as a result of maximum flooding conditions (Greb and Martino, 2005).

The highstand systems tract is identified in this study as an overall upward-coarsening facies succession immediately above the maximum flooding surface (see *Upward-Coarsening Succession*). Multiple high-frequency upward-fining intervals are present within the overall upward-coarsening succession, commonly capped by coals. The HST is terminated by the overlying sequence boundary. In the case of lenticular sandstone elements that have pinched out above the HST, the sequence boundary is placed at the regionally extensive coal capping the succession (**Fig. 13; Sequence B4;** Aitken and Flint, 1994; 1995).

7. APPLICATIONS TO CARBON SEQUESTRATION

7.1. Motivation

In 2003, the Department of Energy (DOE) created seven Regional Carbon Sequestration Partnerships as part of a national plan to mitigate greenhouse gas emissions. The Virginia Center for Coal and Energy Research (VCCER) at Virginia Tech is part of the Southeast Regional Carbon Sequestration Partnership (SECARB), led by the Southern States Energy Board (SSEB). VCCER has been tasked with assessing carbon sequestration potential within the Central Appalachian Basin. Coal is considered a major sink for geologic sequestration of carbon dioxide (Byrer and Guthrie, 1999; Gentzis, 2000; Reichle et al., 1999).

The Central Appalachian Basin contains numerous productive coal-bed methane (CBM) operations. Many CBM operations are approaching maturity, providing large reservoirs for carbon sequestration. Injection of carbon dioxide into coal seams has been used to enhance coal-bed methane recovery, and may increase coal-bed methane reserves by 20 to 40 percent in the Central Appalachian Basin while concurrently storing large volumes of carbon dioxide (Conrad et al., 2007; Pashin et al., 2003).

VCCER, in conjunction with Marshall Miller & Associates (MM&A), is refining estimates of carbon sequestration potential in CBM fields in the Central Appalachian Basin on a field by field basis. This paper presents findings from the Bradshaw CBM field in McDowell County, WV.

7.2. Study Interval

The study interval includes coals of the Pocahontas Formation and Bottom Creek Formation. Coals within the study interval are generally high rank (low-volatile bituminous) and high gas content (**Fig. 21;** Ripepi et al., 2006). Coals of the Lower Pennsylvanian Pocahontas Formation include Pocahontas No. 1 through Pocahontas No. 9 seams. The Bottom Creek Formation unconformably overlies the Pocahontas Formation, and includes eight major coal seams: Upper Seaboard, Greasy Creek, Middle Seaboard, Lower Seaboard, Upper Horsepen, Middle Creek, War Creek, and Lower Horsepen.

7.3. Methodology

7.3.1. Estimates of total coal reserves

Coal thickness was determined by a combination of direct measurement in outcrop (for Pocahontas Formation coals) and subsurface estimates of area under the bulk density curve that fall below 2 g/cm^3. Wells with compromised density logs were removed from total coal thickness calculations.

Two stratigraphic sequences were delineated for mapping coal seams in the study area; 1) Bottom Creek Formation consisting of Upper Horsepen to X coal seams, and 2) Pocahontas Formation consisting of Pocahontas No. 9 to Pocahontas No. 3 coal seams. A composite coal isolith map for Bottom Creek Formation and Pocahontas Formation coals in the Bradshaw CBM field was created using Haliburton's Geographix software (**Fig. 22**).

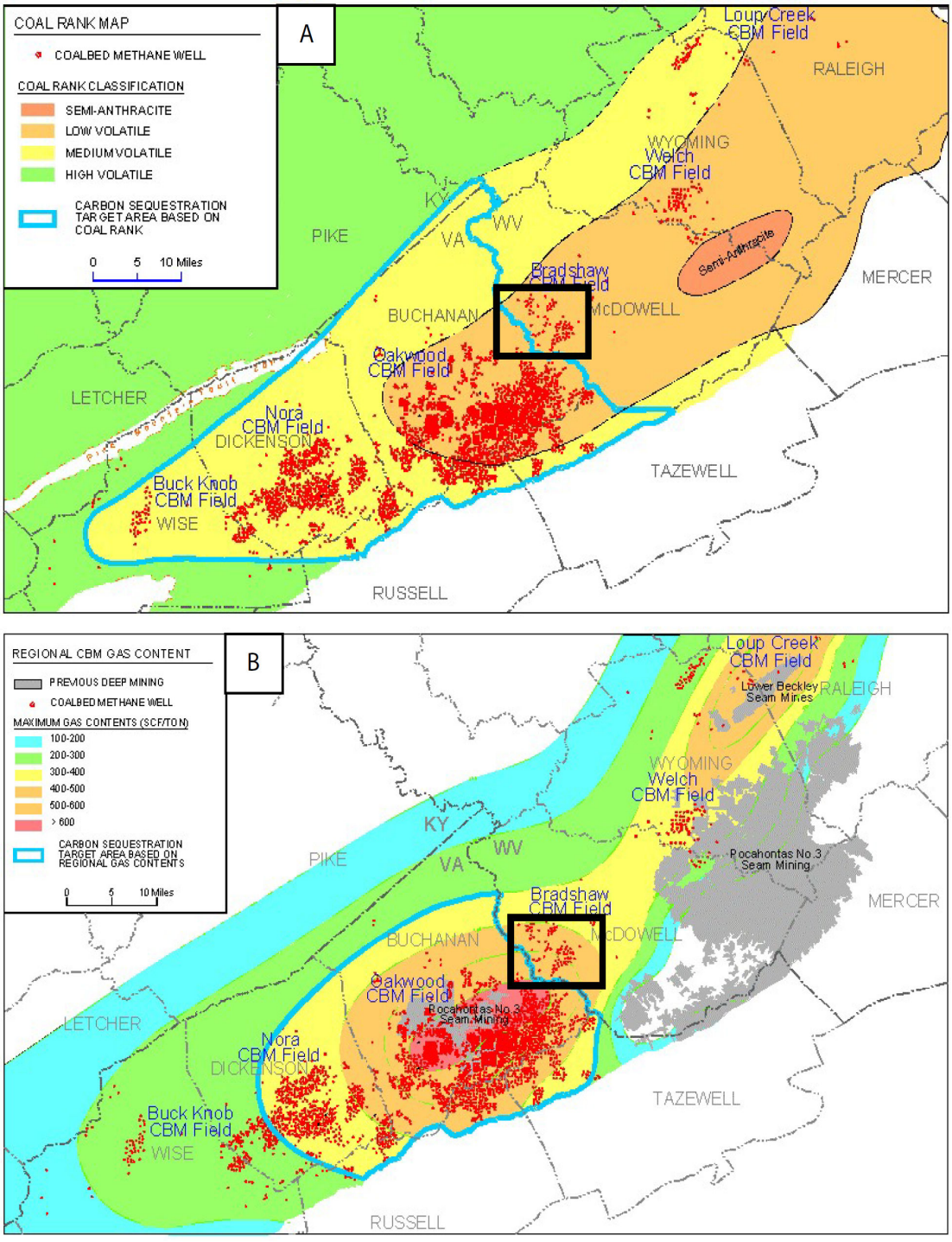

Figure 21. Regional A) coal rank and B) gas content maps of the central Appalachian Basin (area of interest boxed) (modified from Ripepi et al., 2006).

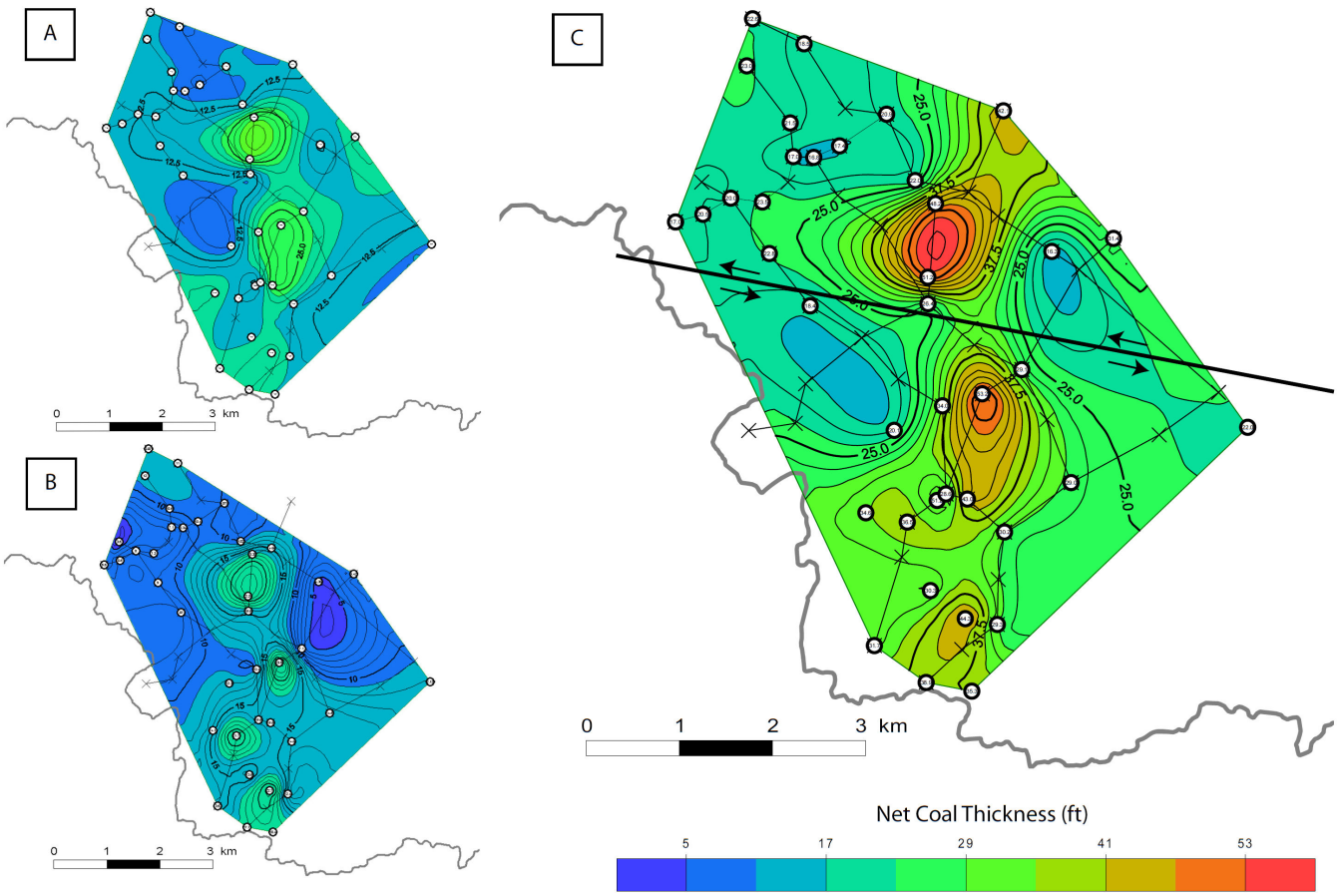

Figure 22. Net coal isolith maps for the Bradshaw CBM field. A) Net coal isolith map for the lower Pennsylvanian Pocahontas Formation. B) Net coal isolith map for the lower Pennsylvanian Bottom Creek Formation. C) Net coal isolith map for the Bottom Creek and Pocahontas Formations. Note left-lateral strike-slip fault displacing coal body.

7.3.2. Calculation of CO_2 storage potential

Methodology for quantification of carbon dioxide storage potential in the Bradshaw CBM field employs a volumetric approach established by the Geologic Society of Alabama (GSA). This method uses a geographic information systems (GIS) based analysis, utilizing net coal isolith and coal rank maps, assumptions of reservoir temperature and storage pressure, and estimates of sorption capacity (Pashin, 2005).

Reservoir temperature and storage pressure were estimated at 74°C and 350 psi, respectively, from similar studies of sequestration potential in CBM fields of the central Appalachian basin (Ripepi et al., 2006).

Previous analysis of sorption isotherms found that coal rank is the primary control on sorption capacity in coals of the Black Warrior Basin (GSA), with higher rank coals generally having higher gas contents. Pashin (2005) developed a sorption-rank relationship for coals in the Black Warrior Basin (**Fig. 23**). Low-volatile bituminous coals in the study area are estimated to average 18 percent volatile matter (Ripepi et al., 2006). Extrapolating the sorption-rank relationship results in a CO_2 sorption capacity estimate of 776 scf/t for low-volatile bituminous coals in the study area (Ripepi et al., 2006). Carbon dioxide storage capacity was calculated from the following equation:

$$CO_2\ Capacity = V_{coal} \times D_{coal} \times SC \times P \times T \qquad (1)$$

where V_{coal} is coal volume (cf), D_{coal} is coal density (t/cf) (2 g/cm^3 = 0.06 t/cf), SC is sorption capacity (cf/t), P is sorption adjustment for pressure (=1.0004), and T is sorption adjustment for temperature (=1.0299) (Ripepi et al., 2006).

7.3.3. Calculation of enhanced coal-bed methane recovery potential

Calculation of enhanced coal-bed methane recovery potential in a coal-bed methane field relies on estimates of gas volumes not likely to be recovered during primary production, thus potentially recoverable during enhanced-recovery operations by sequestering carbon dioxide. Gas-initially-in-place (GIIP) values for coals in the

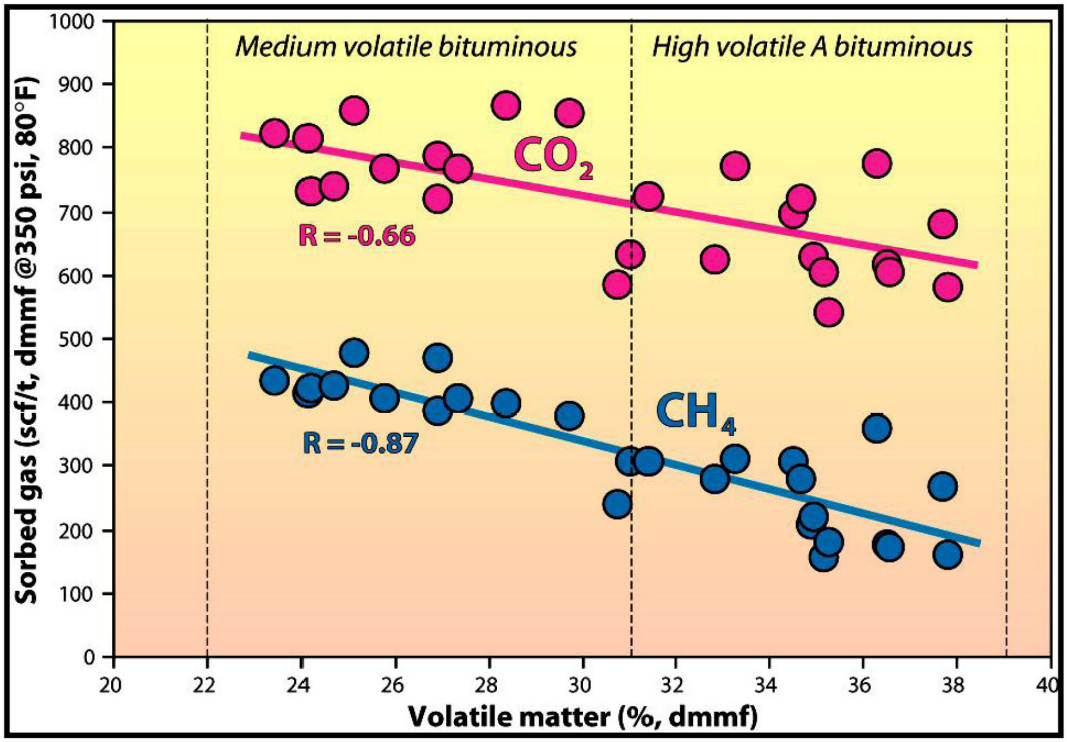

Figure 23. CO2 and CH4 sorption - rank relationship, Black Warrior Basin (from Pashin, 2005).

Bradshaw CBM field were taken from regional gas content maps created by MM&A, with gas contents ranging from 400 to 600 scf/t. For the purpose of calculations, a value of 500 scf/t was used for GIIP. ECBM recovery was calculated from the following equation:

$$ECBM\ Recovery = V_{coal} \times D_{coal} \times GIIP \times RF \qquad (2)$$

where *RF* is the ECBM recovery factor (=25%) (Ripepi et al., 2006). The recovery factor was based on the assumption that 55% of the gas in place would be recovered by primary recovery operations, 20% of the gas in place is unrecoverable residual gas, and the remaining 25% can be recovered using enhanced recovering operations using CO_2 sequestration (Ripepi et al., 2006).

7.4. Results

The determined coal volume, CO_2 storage capacity, and enhanced coal-bed methane recovery potential for the Bradshaw CBM field are presented in Tables 1-3, respectively.

Table 1. Volume of coal (Bcf) in lower Pennsylvanian formations for the Bradshaw CBM field, McDowell County, WV	
Pocahontas Formation	4.18 Bcf
Bottom Creek Formation	3.06 Bcf
Total *(Pocahontas and Bottom Creek Formations)*	**7.05 Bcf**

Table 2. CO_2 storage capacity for the Bradshaw CBM field, McDowell County, WV	
Total Storage Capacity: *(Pocahontas and Bottom Creek Formations)*	**338 Bcf**

Table 3. Enhanced coal-bed methane recovery potential for the Bradshaw CBM field, McDowell County, WV	
ECBM Potential: *(Pocahontas and Bottom Creek Formations)*	**52 Bcf**

7.5. Geologic Controls on CBM and Carbon Sequestration

As coal-bed methane fields in the Central Appalachian basin approach maturity, carbon sequestration and enhanced coal-bed methane has the potential to add significant recoverable reserves and extend the life of these fields while at the same time providing a geologic sink for atmospheric greenhouse gases. The geologic variables controlling the distribution and producibility of coal-bed methane resources are essentially the same as those determining carbon sequestration potential in coal seams (Pashin et al., 2001). These variables include stratigraphy, structural geology, and hydrogeology.

7.5.1. Stratigraphy

Coal forms when plants are deposited in swamps, then submerged rapidly enough to limit oxidation but allow microbial decomposition. In the Pocahontas Formation, these conditions were met in fluvial settings as base level rise resulted in flooding and the formation of backswamps on extensive braided river floodplains. These backswamps were shallow and of a constant depth to allow enough plant mass and its covering of sediment to accumulate as undisturbed peat. This process, known as peatification, continued as decomposing plants were progressively covered with sediments (Rogers, 1994). Once deeply buried, peat underwent the process of coalification, transforming as a function of pressure, temperature and time (Rogers, 1994).

Bohacs and Suter (1997) showed that when peat production and accommodation rate are roughly equal, economically significant coal seams are preserved within the stratigraphic record. Conditions where peat production can match accommodation rate occur twice during a sequence: 1) during base level rise until just before base level

reaches a maximum (maximum flooding surface), and 2) during the decrease in the rate of base level rise following maximum flooding conditions. Laterally extensive coal seams of the Pocahontas Formation occur within upward-fining transgressive facies as well as upward-coarsening highstand facies (**Figs. 8-14**), consistent with the above base level controls on coal preservation. Both allocyclic and autocyclic processes are responsible for the formation and preservation coal seams in the lower Pennsylvanian strata, with

The location of established coal-bed methane resources in the Central Appalachian basin is a function of both the net stratigraphic thickness of coal seams in the basin and depth of coal intervals. The optimal depth window for effective coal-bed methane production is situated between 300 and 1500 meters below the surface (Gale and Freund, 2001; Laenen and Hildenbrand, 2005). The shallower depth limit reflects the need for coal seams to be buried deep enough to ensure sufficient reservoir pressure, while the deeper depth limit is based on the recognition that permeability of coals decrease with increasing depth (Laenen and Hildenbrand, 2005). Coal-beds of the Lower Pennsylvanian Pocahontas and Bottom Creek Formations in the Bradshaw CBM field occur between 300 and 640 meters in depth, well within the optimal depth window for effective coal-bed methane production.

7.5.2. Structural geology

Natural fractures occur in nearly all coal beds, exerting a fundamental control on methane storage and sequestration potential. As coalification progressively changes the molecular structure of coals, a point is reached where thermogenic methane is evolved in

large volumes (Rogers, 1994). Unlike a conventional reservoir where gas occupies free spaces between sand grains, methane is held to the surface of coal by adsorption in numerous micropores (Rogers, 1994). Excess methane that cannot be stored in coal surface micropores is transported by the development of a network of fractures within the coal.

While folds and faults control the distribution and production potential of conventional hydrocarbons, conventional trapping mechanisms play a limited role in coal, which is a self-sourced reservoir (Pashin and Groshong, 1998). The importance of folds and faults in coal-bed methane production and carbon sequestration lies in enhanced fracture permeability. Producing gas from coal relies on the ability to desorb methane from the coal microstrucure, accomplished by reducing reservoir pressure by removing formation water that resides in natural fractures. Coals with fracture enhanced permeability generally have formation water that is readily mobilized. This readily mobilized formation water allows for greater reduction of reservoir pressure, thus making desorption of methane from the coal microstructure easier. Enhanced fracture permeability aids in the sequestration of carbon dioxide in coal seams by providing the surface area needed to rapidly sorb CO_2 into the coal microstructure. However, structural integrity of bounding strata is of greater concern in CO_2 sequestration than in coal-bed methane production, as the cap rock must provide an adequate seal to prevent CO_2 migration from the target reservoir.

The positive correlation between folds, faults, and CBM production rates is well documented in both the Nora and Oakwood Fields of southwest Virginia, where increased CBM production rates have been observed along anticline and monocline

structural features, as well as near faults (Ripepi et al., 2006). A structure contour map reveals the presence of a NW-SE trending anticline, likely providing fracture enhanced permeability to the Bradshaw CBM field (**Fig. 24**). Additionally, a left-lateral strike-slip fault has been identified in the Bradshaw CBM field by operator Equitable Production Company, and is evident on net-coal isolith maps (**Fig. 22**). The Bradshaw field fault is likely part of the Canebrake fault system to the north (**Fig. 25**), and is expected to further enhance fracture permeability.

7.5.3. Hydrogeology

The major hydrogeologic factor affecting coal-bed methane production and sequestration of CO_2 is reservoir pressure (Pashin et al., 2001). Reservoir pressure is a primary determinant of gas sorption capacity in coal (Kim, 1977). The amount of gas that a coal can adsorb varies directly with pressure and inversely with temperature:

$$V = k_o P^{n_o} - bT \qquad (3)$$

where V is volume of gas adsorbed (cm^3/g), P is pressure (atm), T is temperature (^oC), and k_o, n_o, and b are constants (Kim, 1977). Thus for coal-bed methane production, higher initial reservoir pressures result in greater volumes of recoverable resource.

The positive correlation between reservoir pressure and sorption capacity of coal is equally important for carbon sequestration. A study by (Wolf et al., 1999) on sorption of CO_2 in carboniferous coal showed that coal can hold approximately twice as much CO_2 as methane. Other factors influencing sorption capacity include rank, grade, and maceral composition of coal (Bustin and Clarkson, 1998; Lamberson and Bustin, 1993).

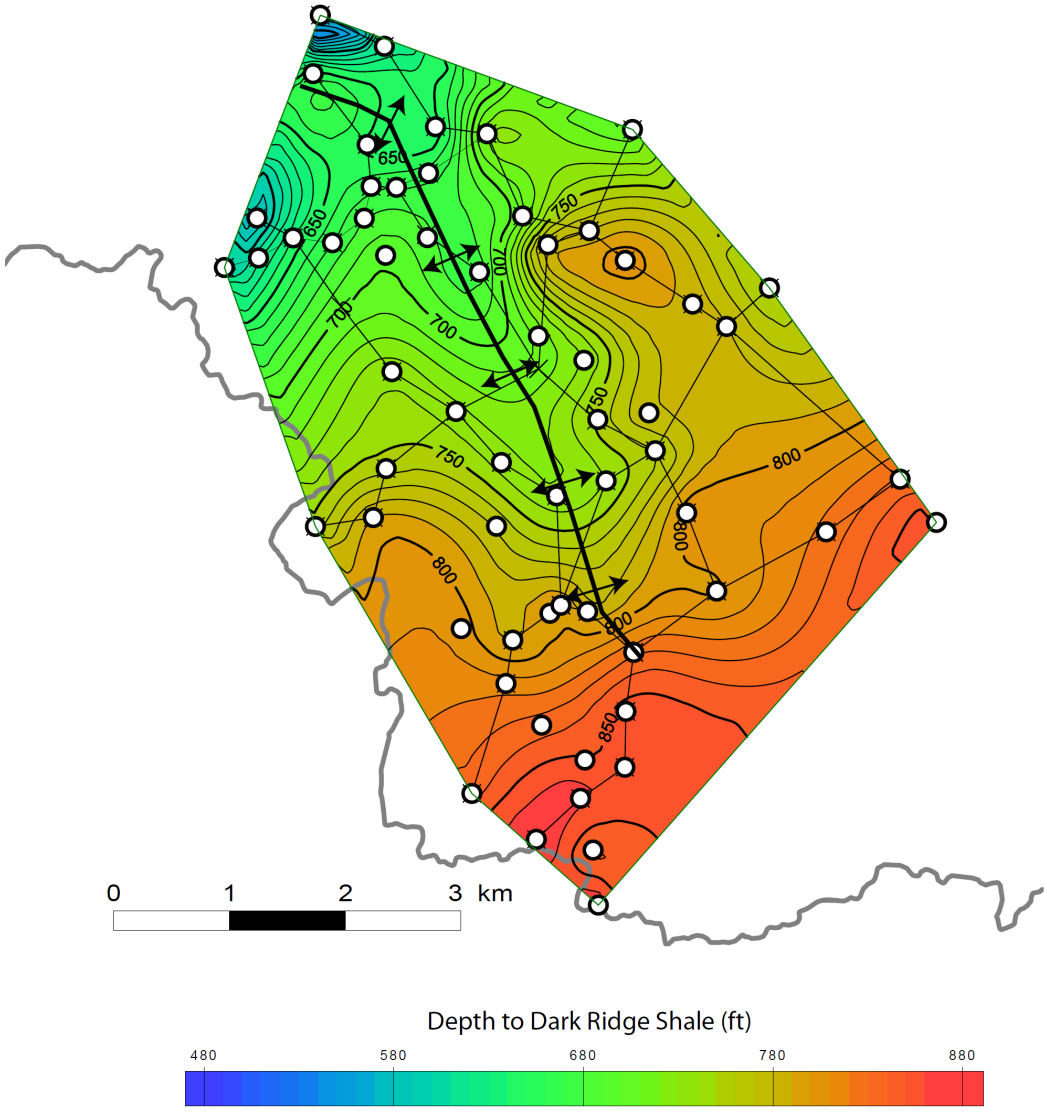

Figure 24. Structure contour map hung on the Dark Ridge Shale for the Bradshaw CBM field. Note NW-SE trending anticline.

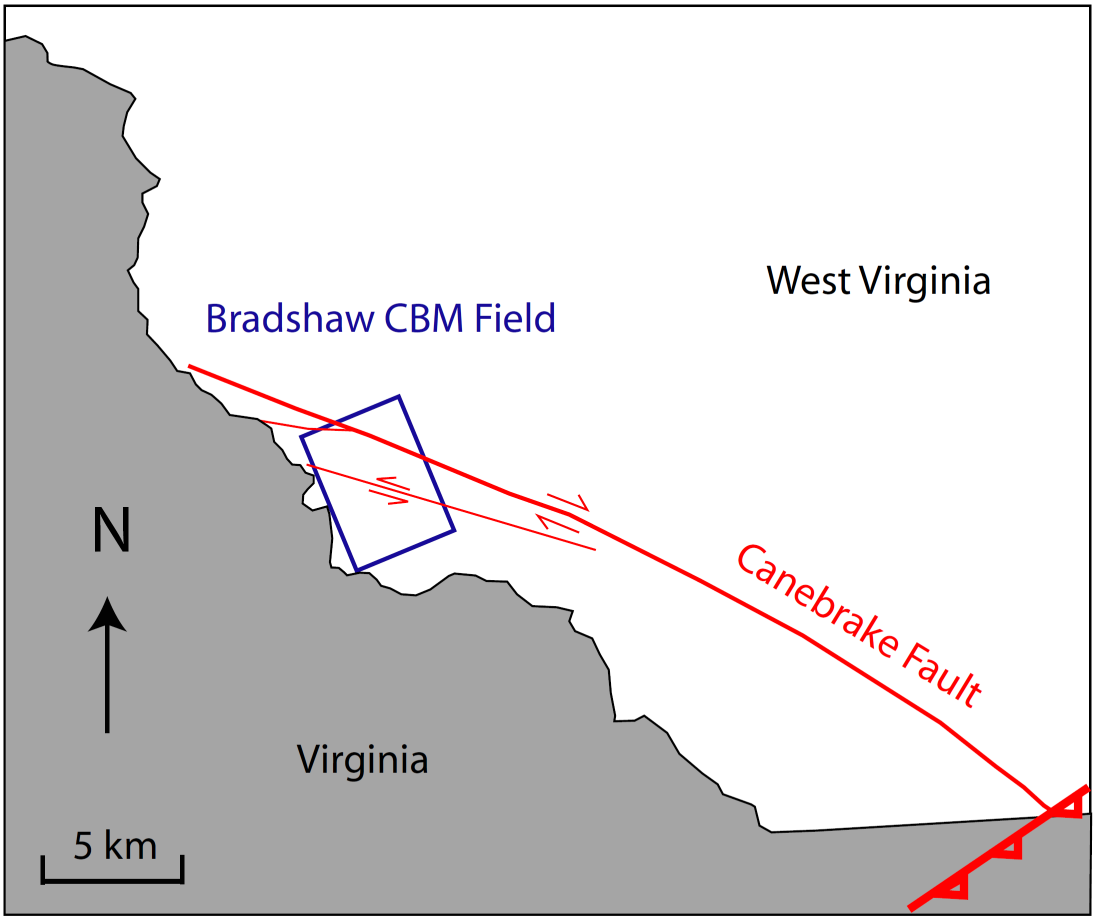

Figure 25. Location of the Canebrake fault system in relation to the Bradshaw CBM field (modified from McLoughlin, 1986).

7.6. CO_2 Storage Capacity and ECBM Recovery Potential in the Bradshaw CBM Field

Results from this study show that CO_2 sequestration in the Bradshaw CBM field shows exceptional promise. Total storage capacity for CO_2 sequestration was determined to be 338 Bcf, or ~19 million metric tons (Mt) (**Equation 1; Table 2**). To put this value into perspective, the nearest CO_2 source is a natural gas processing plant that emits ~2.8 Mt of CO_2 annually. The relatively small (~25 km^2) Bradshaw CBM field has the capacity to sequester all emissions from this processing plant for ~7 years at current emission rates, while at the same time recovering 52 Bcf of additional methane (**Equation 2; Table 3**) worth an estimated $248 million (at $4.77/MMBtu).

While the geology and calculated storage capacities at the Bradshaw CBM field are ideal for sequestration and enhanced coal-bed methane production, coal seams have yet to be validated as a viable sequestration reservoir on a commercial scale. In order for sequestration in coal seams to work, CO_2 breakthrough into producing wells must be kept at a minimum (Ripepi, 2009). A recent small-scale injection test of 1,000 tons of CO_2 into a CBM well in Russell County, VA by Ripepi (2009) was successful, with minimal CO_2 breakthrough occurring (~2.5% of CO_2 initially injected). Larger, commercial-scale injection tests are needed to determine if CO_2 breakthrough into producing wells is controllable during injection of large quantities of CO_2. If it is found that CO_2 breakthrough cannot be controlled at commercial injection levels, sequestration of CO_2 in coal seams would have to occur at the end of the production life for CBM fields (Ripepi, 2009). Additionally, future work taking into account coal adsorption data and CBM production decline curves not available for this study is needed to further refine estimates

of CO_2 storage capacity and enhanced coal-bed methane recovery potential for CBM fields in the central Appalachian Basin.

8. CONCLUSIONS

1. Lower Pennsylvanian coal-bearing strata in the central Appalachian Basin of southern West Virginia were deposited by bedload dominated braided river systems draining two different source terrains: a northerly cratonic source terrain characterized by quartz-rich incised valley fills oriented NE-SW, and a southeastern metamorphic source terrain characterized by sublithic incised valley fills oriented SE-NW.
2. Deposition of the lower Pennsylvanian Pocahontas Formation was influenced by high-magnitude sea-level fluctuations. Sea level lowstand to early transgression is represented by the incision and backfilling of incised valleys with sublithic incised valley fill. Continued transgression resulted in overbank flooding and the formation of backswamps within the fluvial floodplains. During relative sea-level fall, crevasse-splay and progradational deltaic facies developed.
3. Lower Pennsylvanian strata of the Pocahontas and Bottom Creek Formations contain both 3rd- and 4th-order sequences. Third-order composite sequences are built of multiple stacked 4th-order sequences, reflecting major sea level fluctuations. Major, 3rd-order sequences are likely a product of lower-frequency (~2.5 m.y.) orbital eccentricity cycles. Minor, 4th-order sequences are attributed to higher frequency (~400 k.y.) Milankovitch driven glacio-eustacy.
4. Coals within the lower Pennsylvanian Pocahontas and Bottom Creek Formations occur in the transgressive and highstand systems tracts, associated with 4th-order

flooding surfaces and high-frequency deltaic autocycles, respectively. Thus transgressive coal-bed development is attributed to Milankovitch driven glacio-eustacy while highstand coal-bed development is attributed to autocyclic deltaic influences.

5. Geologic controls affecting coal-bed methane production are the same as those governing carbon sequestration potential of coal seams. These controls include stratigraphy, structural geology, and hydrogeology. The Bradshaw CBM field is ideally located, with estimated CO_2 storage capacity of 338 Bcf and enhanced coal-bed methane recovery potential of 52 Bcf worth an estimated $248 million. Further large scale injection tests are needed in the central Appalachian basin to determine the viability of coal seams as sequestration reservoirs and ECBM at a commercial scale.

9. REFERENCES

Administration, E.I., 1994, State coal profiles: DOE/EIA-0576, p. 139.

Aitken, J., and Flint, S., 1994, High-frequency sequences and the nature of incised-valley fills in fluvial systems of the Breathitt Group (Pennsylvanian), Appalachian foreland basin, eastern Kentucky: Incised Valley Systems: Origin and Sedimentary Sequences, p. 3-368.

—, 1995, The application of high-resolution sequence stratigraphy to fluvial systems: a case study from the Upper Carboniferous Breathitt Group, eastern Kentucky, USA: Sedimentology, v. 42, p. 3-30.

Allen, J.L., 1993, Lithofacies relations and controls on deposition of fluvial-deltaic rocks of the upper Pocahontas Formation in southern West Virginia: Southeastern Geology, v. 33, p. 131-147.

Archer, A., and Greb, S., 1995, An Amazon-scale drainage system in the early Pennsylvanian of central North America: The Journal of Geology, v. 103, p. 611-627.

Beuthin, J., 1994, A sub-Pennsylvanian paleovalley system in the central Appalachian basin and its implications for tectonic and eustatic controls on the origin of the regional Mississippian-Pennsylvanian unconformity: Tectonic and eustatic controls on sedimentary cycles: SEPM Concepts in Sedimentology and Paleontology, v. 4, p. 107–120.

Bhattacharya, J., Walker, R., and James, N., 1992, Facies Models: Response to Sea Level Change: Deltas, models for exploration: Houston Geological Society, p. 157-177.

Bodek, R.J., 2006, Sequence stratigraphic architecture of early Pennsylvanian, coal-bearing strata of the Cumberland Block a case study from Dickenson County, Virginia: [Blacksburg, Va. :, University Libraries, Virginia Polytechnic Institute and State University.

Bohacs, K., and Suter, J., 1997, Sequence stratigraphic distribution of coaly rocks: Fundamental controls and paralic examples: Aapg Bulletin-American Association of Petroleum Geologists, v. 81, p. 1612-1639.

Bustin, R., and Clarkson, C., 1998, Geological controls on coalbed methane reservoir capacity and gas content: International Journal of Coal Geology, v. 38, p. 3-26.

Byrer, C., and Guthrie, H., 1999, Appalachian coals: Potential reservoirs for sequestering carbon dioxide emissions from power plants while enhancing CBM production: Tuscaloosa, Alabama, p. 319-327.

Chesnut, D.R., 1996, Geologic framework for the coal-bearing rocks of the Central Appalachian Basin: International Journal of Coal Geology, v. 31, p. 1-4.

Chesnut, D.R., Jr., 1994, Eustatic and tectonic control of deposition of the Lower and Middle Pennsylvanian strata of the Central Appalachian Basin: Concepts in Sedimentology and Paleontology, v. 4, p. 51-64.

Coleman, J., 1976, Deltas: processes of deposition and models for exploration. Continuing Education Publication Company: Inc., Champaign, IL.

Coleman, J., and Wright, L., 1975, Modern river deltas: variability of processes and sand bodies: Deltas, models for exploration, p. 99–149.

Congress, I.G., 1975, Abstracts of papers presented during the Eighth international congress on Carboniferous stratigraphy and geology: VIII International Congress on Carboniferous Stratigraphy and Geology, v. 8, p. 380.
Conrad, J.M., Miller, M.J., and Ripepi, N., 2007, Potential for carbon sequestration in the central Appalachian basin: Air and Waste Management Association Conference.
Davydov, V., Wardlaw, B., and Gradstein, F., 2004, The carboniferous period: A geologic time scale, v. 222, p. 248.
Denning, S.F., 2008, Architectural models for lower Pennsylvanian strata in Dickenson/Wise County, Southwest Virginia a reservior case study: [Blacksburg, Va. :, University Libraries, Virginia Polytechnic Institute and State University.
Dott, R., 1964, Wacke, graywacke and matrix; what approach to immature sandstone classification?: Journal of Sedimentary Research, v. 34, p. 625-632.
Englund, K.J., 1974, Sandstone distribution patterns in the Pocahontas Formation of Southwest Virginia and southern West Virginia: Special Paper Geological Society of America, no, v. 148, p. 31-45.
Englund, K.J., Arndt, H.H., and Henry, T.W., 1979, Proposed Pennsylvanian system stratotype, Virginia and West Virginia : field trip no. 1, ninth International Congress of Carboniferous Stratigraphy and Geology: Falls Church, Va. :, American Geological Institute.
Englund, K.J., and Thomas, R.E., 1990, Late Paleozoic depositional trends in the central Appalachian Basin: U. S. Geological Survey Bulletin, Report: B.
Englund, K.J., Windolph, J.F., Jr., and Thomas, R.E., 1986, Origin of thick, low-sulphur coal in the Lower Pennsylvanian Pocahontas Formation, Virginia and West Virginia: Special Paper Geological Society of America, v. 210, p. 49-61.
Ettensohn, F.R., 2004, Modeling the nature and development of major Paleozoic clastic wedges in the Appalachian Basin, USA: Journal of Geodynamics, v. 37, p. 657-681.
Gale, J., and Freund, P., 2001, Coal-bed methane enhancement with CO2 sequestration worldwide potential: Environmental Geosciences, v. 8, p. 210.
Galloway, W., 1989, Genetic stratigraphic sequences in basin analysis; II, Application to Northwest Gulf of Mexico Cenozoic basin: Aapg Bulletin, v. 73, p. 143-154.
Gentzis, T., 2000, Subsurface sequestration of carbon dioxide—an overview from an Alberta (Canada) perspective: International Journal of Coal Geology, v. 43, p. 287-305.
Gibling, M.R., Saunders, K.I., Tibert, N.E., and White, J.A., 2004, Sequence sets, high-accommodation events, and the coal window in the Carboniferous Sydney Coalfield, Atlantic Canada: AAPG Studies in Geology, v. 51, p. 169-197.
Greb, S., and Chesnut, D., 1992, Transgressive channel filling in the Breathitt Formation(Upper Carboniferous), Eastern Kentucky Coal Field, USA: Sedimentary Geology, v. 75, p. 209-221.
Greb, S., Chesnut Jr, D., and Eble, C., 2004, Temporal changes in coal-bearing depositional sequences (Lower and Middle Pennsylvanian) of the central Appalachian Basin, USA: Coal-bearing strata: Sequence stratigraphy, paleoclimate, and tectonics of coal-bearing strata: American Association of Petroleum Geologists, Studies in Geology, v. 51, p. 89–120.

Greb, S.F., and Chesnut, D.R., 1996, Lower and lower Middle Pennsylvanian fluvial to estuarine deposition, central Appalachian basin: Effects of eustasy, tectonics, and climate: Bulletin of the Geological Society of America [Bull. Geol. Soc. Am.], v. 108.

Greb, S.F., and Martino, R.L., 2005, Fluvial-estuarine transitions in fluvial-dominated successions; examples from the Lower Pennsylvanian of the Central Appalachian Basin: Special Publication of the International Association of Sedimentologists, v. 35, p. 425-451.

Heckel, P., Gibling, M., and King, N., 1998, Stratigraphic model for glacial-eustatic Pennsylvanian cyclothems in highstand nearshore detrital regimes: The Journal of Geology, v. 106, p. 373-384.

Hennen, R., and Gawthrop, R., 1915, Wyoming and McDowell counties: W: Va. Geol. Survey (County Reports), v. 783.

Henry, T., and Gordon Jr, M., 1979, Late Devonian through Early Permian (?) invertebrate faunas in proposed Pennsylvanian system stratotype area: AGI Selected Guidebook Series, v. 1, p. 97-103.

Holz, M., Kalkreuth, W., and Banerjee, I., 2002, Sequence stratigraphy of paralic coal-bearing strata: an overview: International Journal of Coal Geology, v. 48, p. 147-179.

Instruments, G., 2000, Geophysical gamma-ray spectrometer: GRS-2000 Multispec: Operating Manual, v. 2.

Kim, A., 1977, Estimating methane content of bituminous coalbeds from adsorption data: US Bureau of Mines Report of Investigations, v. 8245, p. 22.

Korus, J., Kvale, E., Eriksson, K., and Joeckel, R., 2008, Compound paleovalley fills in the Lower Pennsylvanian New River Formation, West Virginia, USA: Sedimentary Geology, v. 208, p. 15-26.

Korus, J.T., 2002, The lower Pennsylvanian New River Formation a nonmarine record of glacioeustasy in a foreland basin: [Blacksburg, Va. :, University Libraries, Virginia Polytechnic Institute and State University.

Krebs, C., 1916, Raleigh County and the Western Portions of Mercer and Summers Counties.

Laenen, B., and Hildenbrand, A., 2005, Development of an empirical model to assess the CO2-ECBM potential of a poorly explored basin.

Lamberson, M., and Bustin, R., 1993, Coalbed methane characteristics of Gates Formation coals, northeastern British Columbia: Effect of maceral composition: Aapg Bulletin, v. 77, p. 2062-2076.

Mack, G., James, W., and Monger, H., 1993, Classification of paleosols: Bulletin of the Geological Society of America, v. 105, p. 129-136.

Matthews, R., and Frohlich, C., 2002, Maximum flooding surfaces and sequence boundaries: comparisons between observations and orbital forcing in the Cretaceous and Jurassic (65–190 Ma): GeoArabia, v. 7, p. 503-538.

McCarthy, P., and Plint, G., 1998, Recognition of interfluve sequence boundaries: Integrating paleopedology and sequence stratigraphy: Geology, v. 26, p. 387.

McLoughlin, T., 1986, Explanation of the regional tectonic map of the southwestern coal field of Virginia, MSHA/IR-1177, Mine Safety and Health Administration, Norton, VA (USA). Roof Control Dept.

Miall, A., 1985, Architectural-element analysis: a new method of facies analysis applied to fluvial deposits: Earth Science Reviews, v. 22, p. 261-308.
Mitchum, R., 1977, Seismic stratigraphy and global changes of sea level, Part 1: Glossary of terms used in seismic stratigraphy: Seismic stratigraphy: Applications to hydrocarbon exploration: American Association of Petroleum Geologists Memoir, v. 26, p. 205–212.
Mitchum, R., and Van Wagoner, J., 1991, High-frequency sequences and their stacking patterns: sequence-stratigraphic evidence of high-frequency eustatic cycles: Sedimentary Geology, v. 70, p. 131-160.
Myers, K., and Wignall, P., 1987, Understanding Jurassic organic-rich mudrocks—new concepts using gamma-ray spectrometry and palaeoecology: examples from the Kimmeridge Clay of Dorset and the Jet Rock of Yorkshire: Marine clastic sedimentology: London, Graham and Trotman, p. 172–189.
O'Mara, P., and Turner, B., 1999, Sequence stratigraphy of coastal alluvial plain Westphalian B Coal Measures in Northumberland and the southern North Sea: International Journal of Coal Geology, v. 42, p. 33-62.
Pashin, J., Carroll, R., Groshong Jr, R., Raymond, D., McIntyre, M., and Payton, J., 2003, Geologic screening criteria for sequestration of CO2 in coal: quantifying potential of the Black Warrior coalbed methane fairway: Annual Technical Progress Report, US Department of Energy, National Energy Technology Laboratory, contract DE-FC-00NT40927, v. 190.
Pashin, J., and Groshong, R., 1998, Structural control of coalbed methane production in Alabama: International Journal of Coal Geology, v. 38, p. 89-113.
Pashin, J.C., 2005, Sequestration potential of CBM reservoirs in the Black Warrior Basin: SECARB Annual Update Meeting.
Pashin, J.C., Carroll, R.E., and Anonymous, 2002, Influence of coal quality on the carbon sequestration potential of coalbed methane reservoirs in the Black Warrior Basin: Environmental Geosciences, v. 9.
Pashin, J.C., Groshong, R.H., Carroll, R.E., and Anonymous, 2001, Enhanced coalbed methane recovery through sequestration of carbon dioxide; potential for a market-based environmental solution in the Black Warrior Basin: Annual Meeting Expanded Abstracts American Association of Petroleum Geologists, v. 2001.
Plint, A., Eyles, N., Eyles, C., and Walker, R., 1992, Control of sea level change: Facies Models–Response to Sea Level Change, p. 15–25.
Posamentier, H., Jervey, M., and Vail, P., 1988, Eustatic controls on clastic deposition I—conceptual framework: Sea-Level Changes: An Integrated Approach: SEPM, Special Publication, v. 42, p. 109–124.
Powell, J., Thompson, A., Coues, E., and Goode, G., 1875, Exploration of the Colorado River of the West and Its Tributaries: Explored in 1869, 1870, 1871, and 1872, Under the Direction of the Secretary of the Smithsonian Institution, Govt. print. off.
Price, W.A., 1916, Chapter X: Notes on the paleontology of Raleigh, Wyoming, McDowell, and adjacent counties: in Krebs, C.E., Raleigh county and the western portions of Mercer and Summers counties: West Virginia Geological Survey [county reports], p. 663-736.

Quinlan, G.M., and Beaumont, C., 1984, Appalachian Thrusting, Lithospheric Flexure, and the Paleozoic Stratigraphy of the Eastern Interior of North-America: Canadian Journal of Earth Sciences, v. 21, p. 973-996.
Read, J., 1995, Overview of carbonate platform sequences, cycle stratigraphy and reservoirs in greenhouse and icehouse worlds: Milankovitch Sea-Level Changes, Cycles, and Reservoirs on Carbonate Platforms in Greenhouse and Ice-House Worlds: SEPM, Short Course, v. 35, p. 1–102.
Reading, H., and Collinson, J., 1996, Clastic coasts: in Reading, HG, ed., Sedimentary Environments: Processes, Facies and Stratigraphy: Blackwell Science, Oxford.
Reed, J., 2003, Thermal and diagenetic evolution of carboniferous sandstones, central Appalachian basin.
Reed, J., Eriksson, K., and Kowalewski, M., 2005, Climatic, depositional and burial controls on diagenesis of Appalachian Carboniferous sandstones: qualitative and quantitative methods: Sedimentary Geology, v. 176, p. 225-246.
Reger, D., 1926, Mercer, Monroe and Summers Counties: West Virginia Geol: Survey County Rept, v. 963.
Reichle, D., Houghton, J., Kane, B., Ekmann, J., Benson, S., Clarke, J., Dahlman, R., Hendrey, G., Herzog, H., and Hunter-Cevera, J., 1999, Carbon Sequestration, State of the Science: US Department of Energy, Office of Science, Office of Fossil Energy, Washington 1999.
Reineck, H., and Wunderlich, F., 1968, Classification and origin of flaser and lenticular bedding: Sedimentology, v. 11, p. 99-104.
Rice, C.L., 1985, Terrestrial vs. marine depositional model; a new assessment of subsurface Lower Pennsylvanian rocks of southwestern Virginia: Geology, v. 13, p. 786-789.
Rice, C.L., and Schwietering, J.F., 1988, Fluvial deposition in the Central Appalachians during the Early Pennsylvanian: U. S. Geological Survey Bulletin, Report: B.
Ripepi, N., Blacksburg, V., and Karmis, M., 2006, Analysis of Enhanced Coalbed Methane Recovery through Carbon Sequestration in the Central Appalachian Basin, p. 06-058.
Ripepi, N.S., 2009, Carbon dioxide storage in coal seams with enhanced coalbed methane recovery geologic evaluation, capacity assessment and field validation of the Central Appalachian Basin: [Blacksburg, Va. :, University Libraries, Virginia Polytechnic Institute and State University.
Rogers, R., 1994, Coalbed methane: principles and practice, Prentice Hall.
Ruppert, L., and Rice, C., 2000, Coal resource assessment methodology and geology of the northern and central Appalachian Basin coal regions, chapter B: Northern and Central Appalachian Basin Coal Regions Assessment Team, ed.
Ryder, R., 1995, Appalachian Basin Province (067): Gautier, DL, Dolton, GL, Takahashi, KI, and Varnes, KL, eds.
Shanley, K., and McCabe, P., 1994, Perspectives on the sequence stratigraphy of continental strata: Aapg Bulletin, v. 78, p. 544-568.
Van Wagoner, J., Mitchum, R., Campion, K., and Rahmanian, V., 1990, Siliciclastic sequence stratigraphy in well logs, cores, and outcrops.
Van Wagoner, J., Posamentier, H., Mitchum, R., Vail, P., Sarg, J., Loutit, T., and Hardenbol, J., 1988, An overview of the fundamentals of sequence stratigraphy

and key definitions: Sea-Level Changes: An Integrated Approach: SEPM, Special Publication, v. 42, p. 39–45.
Walker, R., 1992, Facies, facies models and modern stratigraphic concepts: Facies Models: response to sea level change, p. 1-14.
Walker, R., and James, N., 1992, Facies models: response to sea level change, Geological Association of Canada St John's.
Wanless, H., and Shepard, F., 1936, Sea level and climatic changes related to late Paleozoic cycles: Bulletin of the Geological Society of America, v. 47, p. 1177-1206.
Weller, J., 1930, Cyclical sedimentation of the Pennsylvanian period and its significance: The Journal of Geology, v. 38, p. 97-135.
Wizevich, M.C., 1992, Sedimentology of Pennsylvanian Quartzose Sandstones of the Lee Formation, Central Appalachian Basin - Fluvial Interpretation Based on Lateral Profile Analysis: Sedimentary Geology, v. 78, p. 1-47.
Wolf, K., Hijman, R., Barzandji, O., and Bruining, J., 1999, Laboratory experiments and simulations on the environmentally friendly improvement of coalbed methane production by carbon dioxide injection, p. 3–7.
Zaitlin, B., Dalrymple, R., and Boyd, R., 1994, The stratigraphic organization of incised-valley systems associated with relative sea-level change: Incised-valley systems: origin and sedimentary sequences, p. 45-60.